

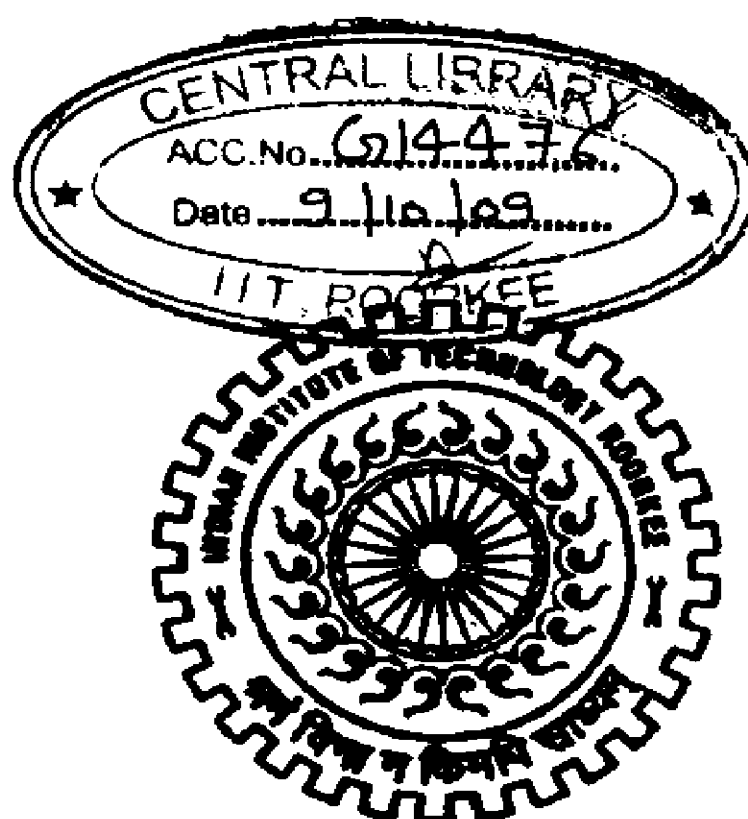
SNOWMELT RUNOFF MODELING IN CHENAB BASIN USING REMOTE SENSING AND GIS

A DISSERTATION

*Submitted in partial fulfillment of the
requirements for the award of the degree
of*
MASTER OF TECHNOLOGY
in
HYDROLOGY

By

HARSH KUMAR



**DEPARTMENT OF HYDROLOGY
INDIAN INSTITUTE OF TECHNOLOGY ROORKEE
ROORKEE-247 667 (INDIA)**

JUNE, 2009

CANDIDATE'S DECLARATION

I hereby certify that the work which is being presented in this dissertation entitled ***"SNOWMELT RUNOFF MODELING IN CHENAB BASIN USING REMOTE SENSING AND GIS"*** in partial fulfilment of the requirement for the award of the degree of **Master of Technology in Hydrology**, submitted in the Department of Hydrology of Indian Institute of Technology, Roorkee is an authentic record of my work carried out during the period from July,2008 to June,2009 under the supervision of **Dr. Manoj Kumar Jain, Assistant Professor**, Department of Hydrology, Indian Institute of Technology, Roorkee and **Dr. Sanjay Kumar Jain, Scientist – E**, National Institute of Hydrology, Roorkee.

The matter embodied in this dissertation has not been submitted by me for the award of any other degree or diploma.

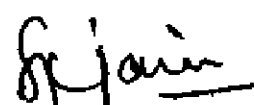


(Harsh Kumar)

Dated: 29/6/09

Candidate's Signature

This is to certify that the above statement made by the candidate is correct to the best of our knowledge.



(Dr. Sanjay Kumar Jain)
Scientist-E,
National Institute of Hydrology,
Roorkee.



(Dr. Manoj Kumar Jain)
Assistant Professor,
Department of Hydrology,
Indian Institute of Technology,
Roorkee.

ACKNOWLEDGEMENTS

It is my profound to express my sincere thanks and heartfelt gratitude to Dr. Manoj Kumar Jain, Assistant Professor, Department of Hydrology, IIT, Roorkee, and Dr. Sanjay Kumar Jain, Scientist - E, National Institute of Hydrology, Roorkee for their tremendous assistance, valuable guidance, suggestions and whole hearted cooperation all through the pursuance of this study "Snowmelt runoff modeling in Chenab basin using remote sensing and GIS".

I would like to express my gratitude to Dr. B.S.Mathur, Eminent Professor, Department of Hydrology for his encouragement and guiding to new horizon of knowledge in the field of hydrology.

My thanks are due to Dr. H.Joshi, Professor and Head, Department of Hydrology Dr. Ranvir Singh, Dr. D.K.srivastava, Dr. D.C.Singhal, Dr. N.K.Goel, Dr. M.Perumal and Dr. D.S.Arya , faculty at Department of Hydrology for rendering all help and heartily cooperation. Their teaching will always remain as an inspiring throughout in my mind and guiding principles in my professional endeavour.

Special acknowledgement must be given to all my seniors and colleagues at Tehri Hydro Development Corporation Limited and Department of Hydrology specially Mr.G.M.Prasad, Mr.R.K.Vishnoi and Mr.Deepak Bisht for encouragement and creating congenial environment during the course of study.

I am thankful to all staff members of Department of Hydrology for their heartily cooperation in every respect.

The author is indebted to his mother and late father for their blessings, constant encouragement and spiritual support throughout my study period.

No words would be enough to express my appreciation to my wife Videeta, sons Ashwin and Ayush for their patience and sacrifices throughout the study period.

Last but no ways least, thanks to the almighty God who has made all this possible.

Date: 29/6/09

Place: Roorkee



(HARSH KUMAR)

CONTENTS

PAGE NO.

	CANDIDATE DECLARATION	i
	ACKNOWLEDGEMENTS	ii
	CONTENTS	iv
	LIST OF TABLES	vi
	LIST OF FIGURES	vii
	ABSTRACT	ix
CHAPTER 1	INTRODUCTION	
	1.1 GENERAL	1
	1.2 GENERAL CHARACTERISTICS OF HIMALAYAN REGION	2
	1.2.1 Physiography and geology	3
	1.2.2 Climate	4
	1.2.3 Snow and ice	5
	1.2.4 River systems	5
	1.2.5 Water resources	9
	1.3 ESTIMATION OF SNOWMELT RUNOFF	9
	1.4 ROLE OF REMOTE SENSING AND GIS	10
	1.5 OBJECTIVES AND SCOPE OF THE PRESENT STUDY	13
CHAPTER 2	REVIEW OF LITERATURE	
	2.1 MODELING OF SNOWMELT RUNOFF	14
	2.1.1 Operational snowmelt models	15
	2.2 SNOWMELT COMPUTATION	18
	2.2.1 Energy balance approach	18
	2.2.2 Degree-day approach or Temperature index approach	21
	2.3 SATELLITE REMOTE SENSING OF SNOW COVER	23
	2.4 SNOWMELT STUDIES FOR HIMALAYAN BASINS	28
	2.4.1 Development of regression relationships	28
	2.4.2 Application of empirical relationships	30
	2.4.3 Application of simulation models	32
CHAPTER 3	STUDY AREA AND DATA USED	
	3.1 THE STUDY AREA	34
	3.2 DATA USED	35
	3.2.1 Topographic data	35
	3.2.2 Hydrometeorological data	35
	3.2.3 Remote sensing data	37
	3.2.3.1 MODIS Data	37

	3.2.3.2	SRTM 90m Digital Elevation Data	39
CHAPTER 4		METHODOLOGY	
	4.1	SNOWMELT RUNOFF MODELING	42
	4.2	SNOWMELT MODEL (SNOWMOD)	44
	4.2.1	Input Data	45
	4.3	SNOW COVERED AREA	46
	4.3.1	Methodology	48
	4.3.1.1	Preparation of Snow cover map	48
	4.3.1.2	Depletion curves	49
	4.4	TEMPERATURE LAPSE RATE	50
	4.4.1	LST Map generation from NOAA-AVHRR Images	53
	4.4.2	Temperature Lapse Rate Estimation	55
	4.5	MODEL VARIABLES AND PARAMETERS	57
	4.5.1	Division of catchment into elevation bands	57
	4.5.2	Precipitation data and distribution	58
	4.5.3	Degree days	60
	4.5.4	Degree Day Factor	61
	4.5.5	Rain on snow	63
	4.5.6	Computation Of different runoff components	64
	4.5.6.1	Surface runoff from snow covered area	64
	4.5.6.2	Surface runoff from snow-free area	66
	4.5.6.3	Subsurface runoff	67
	4.5.6.4	Total runoff	68
	4.5.7	Routing of different components of runoff	68
	4.5.7.1	Routing of surface runoff	68
	4.5.7.2	Routing of subsurface runoff	70
	4.5.8	Efficiency criteria of the model	71
CHAPTER 5		RESULTS AND DISCUSSION	
	5.1	DIVISION OF CATCHMENT INTO ELEVATION BANDS	74
	5.2	SNOW COVER AREA	74
	5.3	LAND SURFACE TEMPERATURE	80
	5.4	APPLICATION OF MODEL	81
	5.4.1	Calibration of model	81
	5.4.2	Simulation of streamflow	82
	5.5	EFFICIENCY CRITERIA OF THE MODEL	83
CHAPTER 6		SUMMARY AND CONCLUSIONS	90
		REFERENCES	92

LIST OF TABLES

TABLE NO.	DESCRIPTION	PAGE NO.
Table 1.1	Major river systems of the Himalayan region and their catchment areas falling in the Himalayas	8
Table 2.1	List of Snowmelt models	16
Table 3.1	Summary of the MOD10A1 product	39
Table 4.1	Raingauge stations used for different bands	59
Table 4.2	Parameter values used in calibration of model	62
Table 5.1	Chenab basin area covered in different elevation band	75
Table 5.2	Model efficiency during calibration period	82
Table 5.3	Model efficiency during validation period	83

LIST OF FIGURES

FIGURE NO.	DESCRIPTION	PAGE NO.
Figure 3.1	Location of study area	35
Figure 3.2	Drainage map of the study area	36
Figure 3.3	Chenab basin with raingauge locations	37
Figure 3.4	DEM of Chenab river basin upto Premnagar	41
Figure 4.1	Steps involved in SNOWMELT model	45
Figure 5.1	Area covered in each elevation zone of the Chenab basin	75
Figure 5.2	Snowcover Area for 2001	76
Figure 5.3	Snowcover Area for 2002	76
Figure 5.4	Snowcover Area for 2003	77
Figure 5.5	Snowcover Area for 2004	77
Figure 5.6	Snowcover Area for 2005	78
Figure 5.7	Snowcover depletion curves for Chenab basin	78
Figure 5.8	Snow covered depletion in bands 4, 5, 6 and 7	79
Figure 5.9	Lapse rate estimation from MODIS LST maps	80
Figure 5.10	Temperature Lapse rate for Chenab basin	81
Figure 5.11	Comparison of observed and simulated hydrographs for the calibration period (2000-01) for the study area	85

Figure 5.12	Comparison of observed and simulated hydrographs for the calibration period (2001-02) for the study area	86
Figure 5.13	Comparison of observed and simulated hydrographs for the calibration period (2002-03) for the study area	87
Figure 5.14	Comparison of observed and simulated hydrographs for the calibration period (2003-04) for the study area	88
Figure 5.15	Comparison of observed and simulated hydrographs for the calibration period (2004-05) for the study area	89

ABSTRACT

Snow is a great resource for water particularly for Himalayan Rivers. Although seasonal snow cover is an important parameter in the hydrological regime of a basin, its contribution is confined to the spring season when snow-melt and base-flow constitute two components of the discharge. Once the summer sets in, it is the exposed glacier ice in the ablation zone which is the main contributor to the melt along with monsoon rainfall.

The present study is primarily carried out for assessment of streamflow in the Chenab River up to Premnagar. In the study Terra MODIS satellite data has been used for mapping the snow cover area (SCA). The lapse rate has been estimated using the LST maps generated from the thermal bands of the satellite data. A methodology to produce daily SCA directly from Terra MODIS snows cover map products (MOD10A1) is presented. The study catchment is divided into nine elevation zones and snow cover has been computed for these elevation zones using MODIS data. On the basis of SCA, snow cover depletion curves have been prepared. The Snow cover depletion curves vary significantly from year to year. It was observed that the snowmelt starts in the month of March while after August snow cover accumulation starts. The upper part of the basin remains snow covered and lower part remains snow free throughout the year. Snow covered area varies between 10% and 80% in the whole basin depending on time of the year.

Study reveals that there exists an inverse linear correlation between LST and elevation. Using this property, the lapse rate for different seasons has been computed.

Simulation has been carried out taking snow cover area, lapse rate and meteorological data using snowmelt runoff model. Available data of five years was split into two parts; one is used for calibration purpose (2000-01, 2001-02, 2002-03) and the remaining data of two years (2003-2004, 2004-2005) for model validation. During calibration period, it is noticed that for all the three years the daily discharge simulated with efficiency ranging from 0.84 to 0.92 and difference in volume ranging from 1.57% to 7.26%, which indicates good to very good performance of the model for all the years. The calibrated model was applied to independent data set for years 2003-2004 and 2004-2005 to check the applicability of the model. The model could reproduce independent data sets with efficiency between 0.81-0.91 comparable to that of calibration period indicating applicability of the model to simulate runoff in study basin. The seasonal distribution of streamflow indicates that about 60% of annual flows are generated during the summer season and about 75% of this summer flow is obtained from snowmelt. SNOWMOD, a temperature index based runoff model worked well in the study basin with limited data. Such estimates are useful for planning and management in this basin.

1.1 GENERAL

Stream flow representing the runoff phase of the hydrologic cycle is the most important basic data for hydrologic studies. The first and foremost requisite for the planning of water resources development is accurate data of stream flow, or in other words, the surface runoff for a considerable period of time so as to determine the extent and pattern of the available supply of water. The practical objective of hydrologic analysis is to determine the characteristics of the hydrograph that may be expected for a stream draining any particular watershed. There is a great need of proper assessment of mountain water resources and their proper utilization.

More than half of the humanity relies on the fresh water that accumulates in mountains for drinking, domestic use, irrigation, hydropower, industry and transportation. Rapid and increasing changes in mountain landscapes, and increasing demands on mountain resources, have many impacts on fresh water availability. Fresh water has already become a scarce resource in many parts of the world. Mountains are expected to satisfy the greater part of this growing demand of fresh water. In general, mountains are treated as a resource of water because all the important rivers of the world originate from mountains. Mountain areas constitute a relatively small proportion of river basins, yet they provide significant part of the river flows downstream. There has been very limited monitoring of hydrological data in mountainous areas. An inadequate knowledge of the hydrology of

mountainous areas and poor management of water resources can result in serious degradation of water quantity and quality.

The mountains cover a large portion of the earth surface. As the mean altitude of the land area of the earth is 875 m above sea level, and therefore over 28% of the land areas are above 1,000 m. In these high mountains, it is estimated that 10 to 20% of the total surface area is covered by glaciers while an additional area ranging from 30 to 40% has seasonal snow cover. Out of the total mountain glaciers, central Asian Mountains contain about 50% of the glaciers, a large portion of which drain into the landmass of Indian sub-continent. There are of course variations in depths of snow and ice from place to place depending on the location. Snow and glaciers are the reservoirs with vast storage of fresh water. Snow forms a natural reservoir, storing water for weeks, months or season. If it is properly harnessed it can be used for water supply, agriculture, industry and energy production.

1.2 GENERAL CHARACTERISTICS OF HIMALAYAN REGION

The word Himalaya is a compound of Sanskrit words, "hima" for snow and "alaya" for abode, referring to the lofty range between the Indo-Gangetic plain and the Tibetan plateau. It extends nearly 2,400 km in a vast southerly arc between the blend of the Indus marked by Nanga Parbat (8,125 m) on the west to the Brahmaputra blend around Namcha Barwa (7,755 m) in the east. The Himalayan range is the loftiest mountain complex on earth with 31 peaks exceeding 7,600 m in height. The extreme elevation and rugged relief are the result of rapid mountain-building forces and vigorous erosion processes. In places, they are traversed by

extremely deep river gorges resulting in great vertical contrasts over very short horizontal distances. (Mountain Forum Newsletter, 1999)

1.2.1 Physiography and geology

The Himalayas is the highest and youngest mountain system of the world, on the northern edge of the Indian subcontinent. The width of this mountain system is variable, being broadest in Kashmir (about 400 km.) and narrowest in Sikkim (about 160 km.). Based on its geological and geomorphological history, the system is divisible into three well-recognized transverse zones separated by distinct escarpments or fault lines. From west to east, these zones are further divisible into three sectors. These are referred to as Western Himalayas between the Indus and the Sutlej rivers, comprising the States of Jammu and Kashmir and Himachal Pradesh; Central Himalayas, between the Satluj River and Singalila range (dividing range between Nepal and Sikkim) formed of Uttrakhand and Eastern Himalayas formed of Sikkim, Bhutan and Arunachal Pradesh. The Indian Himalayan region, which is more than 2,800 km in length and 220 to 300 km wide, is spread over the states of Jammu & Kashmir, Himachal Pradesh, Sikkim, Arunachal Pradesh, Nagaland, Manipur, Mizoram, Tripura, Meghalaya, and a part of Assam, along with eight districts of Uttrakhand and one district of West Bengal.

The landscape of Himalayas is founded on an immature geology and on unconsolidated rock-systems. The Siwaliks are the youngest part of the mountain system. The Siwaliks are composed of tertiary sand stones and shales. The thick Upper Siwaliks are made of conglomerates and the Lower Siwaliks beds are formed of soft and hard stones. North of the Siwaliks rise the formidable ranges of the Outer

Lesser Himalaya. These extremely rugged ranges looking down on the Siwaliks are thickly forested. The rocks in lesser and Central Himalayan zone are mainly sedimentary low grade metamorphosed and of igneous origin. The Himalayas have a wide range of parent material and the soils thus have also developed varying characteristics.

1.2.2 Climate

The Himalayan region has large variations in the topography, elevation and location resulting in great contrasting climates from region to region. In general the entire western Himalayan region tends to be semi-arid and/or subhumid. Only the windward slopes of the southern edge are wet, especially between 900 and 2000 m. Here the Middle Himalayas and the Siwaliks have a mean rainfall between 500 and 1000 mm. In the Siwaliks and Middle Himalayas precipitation occurs largely during summer and monsoon months whereas the greater amount of precipitation occurs in the form of snow in the Great Himalayas in the winter months. There is a great variation of temperatures between summer and winter in this region. In July the maximum temperature ranges from 26°C to 29°C in the Siwaliks, in the Middle Himalayas it is between 21°C and 26.5°C and in the Great Himalayas the mean temperature is less than 21°C. In January the western Himalayan region registers a mean temperature of less than 4°C. The higher regions experiences more snow in winter.

1.2.3 Snow and ice

Snow cover is an important component of the hydrologic cycle. A significant part of the earth is covered by snow for at least a portion of the year, producing a substantial change in surface characteristics from those exhibited when snow is absent. About 10% of the earth's surface, $15 \times 10^6 \text{ km}^2$, is covered by polar ice caps and glaciers (Singh and Singh, 2001). The Himalayas contains over 50% of permanent snow and ice fields outside the Polar Regions. This region covers an area of 4.6 million km^2 above 1500 m, 0.56 million km^2 above 5400m and 3.2 million km^2 above 3000 m . The upper catchment of the Himalayan basins is covered by seasonal snow during winters. For example average snow and glacier contribution in the annual flows of Chenab river at Akhnoor was estimated to be 50% and that for Ganga at Devprayag was about 30% (Singh et al., 1997). The accumulated snow in the Himalayan basin becomes an important source of streamflow during the summer time.

1.2.4 River systems

The Himalayas are the source of a large number of rivers, which ensure all the year round availability of water, i.e., they are perennial in nature. Since, agriculture in India is main source of livelihood, therefore, water resources generated in the Himalayas are considered as a boon to the country.

The Indian Himalayan glaciers are broadly divided into the three-river basins of Indus, Ganga and Brahmaputra. The Indus basin has the largest number of glaciers (3,538), followed by the Ganga basin (1,020) and Brahmaputra (662). Researchers

have estimated that about 17 percent of the Himalayas and 37 percent of Karakorum is presently under permanent ice cover. The principal glaciers of this region are Siachen 72 km; Gangotri 26 km; Zemu 26 km; Milam 19 km and Kedarnath 14.5 km. A variety of climates are the beauty of the Himalayan region. The extreme relief of the Himalayas produces marked changes in air masses crossing the region and results in a complex mosaic of "topo-climates" determined by variations in slope, aspect and relative altitude. These range from the sub-tropical climates in the southern plains, to the temperate climate of the middle hills and Alpine (or polar) climates in the high mountains. The main controls on climate are weather systems moving in from the south-east during the summer and from the west in winter. The summer monsoon normally commences in mid-June and lasts until mid-September. The mountain ranges block the northward advancement of the monsoon causing widespread and intense rainfall on southern slopes, whereas on the lee of the mountain ridges, drier conditions prevail. Delayed onset of the monsoon decreases precipitation along the Himalayan arc from east to north-west. There is also a general decrease from south to north with each successively higher mountain range, featuring windward maxima and leeward rain-shadows, which culminate in the high-altitude aridity of the Tibetan plateau. The western Himalayas get more precipitation from the westerly winds during November to April. There is a large variation in the annual average precipitation in the Himalayas. The southern slopes of the Eastern Himalayas experience some of the highest annual rainfall totals on Earth while other areas receive as low as 50 mm a year. Mean daily air temperature is low in January and rises during the pre-monsoon period (February to May) with maximum daily temperature in late May or early June while post-monsoon (October to January) mean daily air temperatures generally decline. Himalayan glaciers form a unique

reservoir that supports mighty perennial rivers such as Indus, Ganga and Brahmaputra, which are the lifelines of millions of people. Recently the geologists of Geological Survey of India (GSI) counted 5,218 glaciers in the Himalayas. It is estimated that 33,200 km² of the Himalaya is glaciated and glaciers occupy about 17 percent of the total mountainous area of the Himalaya while an additional area ranging from 30-40 percent has seasonal snow cover. Meltwater draining from these ice and snowfields is important in regulating the hydrology of the Indian sub-continent. Though it contributes only to 5 percent of total runoff, it releases water in the dry season.

Gradual shift of the snowline due to progressive increase in atmospheric air temperature and release of the water from snow and ice melting makes the water level constant in Himalayan Rivers.

Broadly rivers originating from the Himalayan region can be grouped in three main river systems; the Indus, the Ganga and the Brahmaputra. The rivers that originate and drain through Himalayas are given in Table 1.1. The most important river system of the Himalayan region, which is also the most important system of the country, is the Indus system. It flows from the Tibetan plateau, through India and Pakistan to the Arabian sea (Indian Ocean). Rivers Shyok, Shigar and Gilgit join it in Jammu and Kashmir. The important tributaries, including the Jhelum, Chenab, Ravi, Beas and Satluj join it after entering Pakistan. About 90% of the mean annual flow into the Indus basin originates in the front ranges and high mountains of the Hindu Kush, Karakorum and western Himalayas.

Table 1.1: Major river systems of the Himalayan region and their catchment areas falling in the Himalayas (Singh and Singh, 2001)

S. No.	River	Catchment area in Himalayas (km ²)
A. Indus System		
1.	Indus	268,842
2.	Jhelum	33,670
3.	Chenab	27,195
4.	Ravi	8,029
5.	Beas	14,504
6.	Satluj	56,500
B. Ganga System		
7.	Ganga	23,501
8.	Yamuna	11,655
9.	Ramganga	6,734
10.	Kali	16,317
11.	Karnali	53,354
12.	Gandak	37,814
13.	Kosi	61,901
C. Brahmaputra System		
14.	Brahmaputra	256,928
15.	Teesta	12,432
16.	Raidak	26,418
17.	Manas	31,080
18.	Subansiri	18,130
19.	Luhit	20,720

1.2.5 Water resources

There is very limited scientific information available for Himalayan water resources. This is due to very difficult terrain and hence insufficient network of observations for both precipitation and streamflow measurements. However, the available estimates show that the water yield from high Himalayan catchments is roughly two times as compared to the catchment located in peninsular India. It is believed that this is mainly due to additional inputs from snow and ice melt contributions for the Himalayan Rivers. Various investigators have estimated the water resources of the Himalayan region. It is reported that the specific runoff in the Himalayas is at a maximum in an altitude belt of considerable human activity - 1500 to 3500m and this is about $515 \text{ km}^3/\text{yr}$ from the upper mountains and evaluated that $400\text{-}800 \text{ km}^3/\text{yr}$ flows down as meltwater contributions from the snow and glacier fields in the high mountain region as against earlier conservative estimates of $200 - 500 \text{ km}^3/\text{yr}$.

1.3 ESTIMATION OF SNOWMELT RUNOFF

The Himalayan regions are very young, highly fragile and unstable. Hydrological problems of the western Himalayan region are different than those of plain areas due to variation in topography, climate, landuse and soil characteristics. Rapid population growth and industrialization are leading to major changes in landuse and water utilization of the region. The need for food, fiber, shelter and energy has caused many watersheds to undergo rapid landuse changes, deforestation

and urbanization. This is affecting hydrological characteristics of the Himalayan basins.

The majority of rivers originating from the Himalayas have their upper catchment in the snow covered areas. The solid precipitation results in temporary storage and the melt water reach the river in the melt season. The snow accumulation in Himalayas is generally from November to March, while snowmelt is from April to June. During April to June, snowmelt is the predominant source of runoff and during July to September it forms a significant constituent of melt. The snowmelt runoff modeling is of vital importance in forecasting water yield. Snow and glacier melt runoff is very important particularly in the lean season and it plays a vital role in making perennial nearly all the rivers originating in Himalayas perennial. The contribution of the snow and glacier melt in annual flows of Himalayan rivers at potential project site is not available. Further, the extent of snow cover and its distribution with time is not available for the Himalayan region. Such information is necessary to solve the hydrologic problems of this region. There is great need to develop simple and systematic hydrological models considering rain and snowmelt inputs based on the limited data availability for this region.

1.4 ROLE OF REMOTE SENSING AND GIS

Measurements of snow cover in the mountainous basins are difficult due to harsh climate, complex accessibility and poor communication facilities. With the advent of remote sensing and GIS, this offers exceptional opportunity to assist in resource inventory, integration of data and as a mechanism for analysis.

Potential application areas of remote sensing and GIS in mountain environment include snow cover analysis, terrain analysis, mountain hazard mapping, watershed management and accessibility analysis. With the advent of modern earth resources/monitoring satellites, considerable data on the Himalayan region's natural resources are now available. Advances in satellite image processing and computer analysis have made it possible to evolve a realistic, accurate and uniform database for hydrological studies. Integration of biophysical and socio-economic data can be made in the GIS environment and can be used to develop a good database for the difficult terrain. Contrary to the conventional approach, these tools enable the combination of multi-spectral spatial data and their presentation in a reasonable understandable map format.

Conventional methods have limitations in the monitoring of snow covered area in the Himalayan basins because of inaccessibility. Because of the difficulty of making field measurements in snow covered mountainous regions, remote sensing is perhaps the only means of measuring snow cover extent and properties. Fresh snow has a very high reflectivity in the visible wavelengths; however, it decreases as the snow ages. The reflectivity of snow is dependent on many snow characteristics like shape and size of snow crystals, liquid water content (especially of the near surface layers), impurities in the snow, depth of snow, surface roughness etc. In addition, the solar elevation and azimuth also influences the spectral reflectance to a large extent (Hall and Martinec, 1985).

At present the visible, near IR and thermal IR data from various satellite (Landsat, IRS, NOAA) are being used operationally for mapping the areal extent of snow cover in the Himalayan basins. Visible and near infrared wavelengths, because

they do not penetrate far into the snowpack, mainly provide information about the surface of the snowpack.

Data requirements vary with the geographical area, the type of model and the output requirements. The use of hydrological models for large watersheds and the shortage of good ground based data sources have hydrologists to make increasing use of remotely sensed data. As the scale of hydrological models increases to provide interaction with general circulation models and regional climate models, hydrologists must turn to the world-wide coverage provided by satellites. Precipitation is undoubtedly the most important input data for hydrological models and yet, at the moment, it can be estimated from satellite data only in special circumstances with limited accuracy. In cold regions, the areal extent of snow cover is measured relatively easily at visible and infrared frequencies. Areal extent may be measured to within 20-30m using IRS, Landsat TM or SPOT images although this is at restricted return periods and in cloud-free conditions only. Hydrological processes such as interception, infiltration and runoff depend upon distributed catchment characteristics such as elevation, slope, aspect, vegetation cover and soil type. Land cover is a useful surrogate for many of these characteristics and can be accurately estimated by classification of data from optical sensors. Techniques are now becoming available to use satellite data to provide areal estimates of skin temperature, cloud cover/sunshine duration and surface albedo and to compute evapotranspiration from different land covers.

The role of remote sensing in runoff calculation is generally to provide a source of input data or as an aid for estimating equation coefficients and model parameters. Experience has shown that satellite data can be interpreted to derive thematic information on land use, soil, vegetation, drainage, etc which, combined

with conventionally measured climatic parameters (precipitation, temperature etc) and topographic parameters height, contour, slope, provide the necessary inputs to the hydrological models. The system provides efficient tools for data input into database, retrieval of selected data items for further processing. The use of remote sensing and GIS is applicable in rainfall runoff, soil erosion, snowmelt runoff and groundwater modeling. The land cover maps derived by remote sensing are the basis of hydrologic response units for modelling units.

1.5 OBJECTIVES AND SCOPE OF THE PRESENT STUDY

The foremost objective of the study is

1. Generation of geo-data base of Chenab river basin.
2. Processing of remote sensing data to derive snow cover.
3. Assessment of Lapse rate using land surface temperature maps.
4. Snowmelt runoff modeling using SNOWMOD model.
5. Assessment of stream flow.

The main objective of the present work is application of snowmelt runoff model for a Himalayan basin. This chapter presents a review of relevant literature for snowmelt/rainfall modeling. A section is also devoted to the application of remote sensing in snow studies. Snowmelt studies carried out for the Himalayan basins have been reviewed and presented.

2.1 MODELING OF SNOWMELT RUNOFF

Hydrologic simulation models that include snow are generally divided into three basic components namely the snow cover, a precipitation-runoff relationship and a runoff distribution and routing procedure. Snowmelt runoff simulation models generally consist of a snowmelt model and a transformation model (WMO, 1996). The snowmelt model generates liquid water from the snowpack that is available for runoff. The transformation model is an algorithm that converts the liquid output at the ground surface to runoff at the basin outlet. The snowmelt and transformation models can be lumped or distributed in nature. Lumped models consider whole catchment as a single unit and use one set of parameter values to define the physical and hydrological characteristics. Distributed models attempt to account for the spatial variability by dividing the basin or catchment into sub-areas and computing snowmelt runoff for each sub area independently with a set of parameters corresponding to each of the sub-areas. Generally distributed models use one of the following general approaches to sub-divide a basin:

- (i) Elevation zone or band
- (ii) Basin characteristics such as slope, aspect, soil, vegetation etc. and
- (iii) A fixed or variable length, two or three-dimensional grid.

Lumped and distributed models are classified further by their use of energy balance approach or temperature index approach to simulate the snowmelt process.

2.1.1 Operational snowmelt models

Many models have been created around the world over four decades to describe snowmelt runoff. List of Snowmelt models is elaborated in Table 2.1. These can be divided into two categories, statistical and physical. In turn, these models can be applied in a lumped or distributed manner. The two most common ways of subdividing an area of interest for snowmelt modeling is into elevation zones, or into grid squares.

When precipitation falls as snow it accumulates in the basin and snowpack is developed. Conceptually snowmelt runoff models are rainfall-runoff models with additional component or routines added to store and subsequently melt precipitation that falls as snow. Some snowmelt runoff models are purpose built and are not intended for use in non snowy environments, though they have to make some allowance for precipitation which falls as rain during the melt season. In general, the part of the model which deals with snowmelt has to achieve three operations at each time step.

- Extrapolate available meteorological data to the snowpack at different altitude zones

Table 2.1: LIST OF SNOWMELT MODELS

Model Name	Country of Origin	Reference
NWSRFS (National Weather Service River Forecast System)	USA	Anderson (1973)
HBV (Conceptual Runoff Model for Swedish Catchments)	Sweden	Bergström (1975)
SRM (Snowmelt Runoff Model)	Switzerland	Martinec (1975)
Point Energy/Mass Balance Model	USA	Anderson (1976)
MOEHYDRO2 (Comprehensive Watershed Model)	Canada	Logan (1976)
GAWSER (Guelph Agricultural Watershed Storm-Event Runoff Model)	Canada	Ghate and Whiteley (1977)
UBC (University of British Columbia Watershed Model)	Canada	Quick and Pipes (1977)
WRB (Water Resources Branch Model)	Canada	Kite (1978)
SHE (Systems Hydrologique European Snow Model)	France	Morris and Godfrey (1978)
IHDM (Institute of Hydrology Distributed Model)	UK	Morris (1983)
PRMS (Precipitation-Runoff Modeling System)	USA	Leavesley et al. (1983)
HSP-F (Hydrologic Simulation Program-Fortran)	USA	Johanson et al. (1984)
USDAHL-74 (Revised Model of Watershed Hydrology)	USA	WMO (1986)

SCS (SCS Snowmelt Model)	USA	WMO (1986)
SWMM (Storm Water Management Model)	USA	WMO (1986)
USGS (U.S. Geological Survey Model)	USA	WMO (1986)
QFORECAST (Continuous Simulation and Real-Time Forecast Model)	Canada	WMO (1986)
CEQUEAU	Canada	WMO (1986)
ERM (Empirical Regressive Model)	Czechoslovakia	WMO (1986)
NEDBOR-AFSSSTROMNINGSMODEL (Rainfall -Runoff Model v. II)	Denmark	WMO (1986)
TANK (Tank Model with Snow Model)	Japan	WMO (1986)
YETI	Czechoslovakia	WMO (1986)
SCHNEE	GDR	WMO (1986)
WSRM (Winter Season Runoff Model)	Poland	WMO (1986)
HRO (Hydro Resources Optimization)	USA	WMO (1986)
GMTs-1 (Model of Snowmelt Formation of Lowland Rivers)	USSR	WMO (1986)
GMTs-2 (Model of Snowmelt Formation in a Mountainous Basin)	USSR	WMO (1986)
GMTs-3 (Model of Snowmelt-Rainfall Runoff Formation)	USSR	WMO (1986)
HEC-1 (Hydrologic Engineering Center-1)	USA	USACE (1990)
SSARR (Streamflow Simulation and Reservoir Regulation)	USA	USACE (1991)
SLURP(Simple Lumped Reservoir Parametric Model)	USA	Kite(1995)
SWAT(Soil Water Assessment Tool)	USA	Arnold et al.(1998)

- Calculate rates of snowmelt at different points, and
- Integrate snowmelt over the concerned effective area of the basin and estimate the total volume of new melt water.

The melt water and rainfall, if any, is then routed to the basin outlet. In the next time step the model has to take into account of changes in snow-covered area because there is general depletion of snow covered area with time. A snowmelt runoff model has been developed at NIH for a Himalayan basin. The structure of the model and algorithms used are discussed in brief in the following sections.

2.2 SNOWMELT COMPUTATION

The snowmelt component of snowmelt runoff simulation models generally takes the form of an energy balance or a temperature index to simulate the process of melting. The first approach is known as energy budget or the energy balance approach and the second is the temperature index or degree-day approach. These approaches are discussed below:

2.2.1 Energy balance approach

The energy balance or heat budget of a snowpack governs the production of meltwater. This method involves accounting of the incoming energy, outgoing energy, and the change in energy storage for a snowpack for a given period of time. The net energy is then expressed as equivalent of snowmelt. The energy balance equation can be written in the form (Anderson, 1973).

$$\Delta Q = Q_n + Q_e + Q_h + Q_g + Q_m \quad (2.1)$$

where:

Q_n	=	net radiation (long and short wave)
Q_e	=	latent heat transfer
Q_h	=	sensible heat transfer
Q_g	=	ground snow interface heat transfer
Q_m	=	heat transfer by mass changes (advected heat)
ΔQ	=	change in heat storage

In the above energy balance equation, different components of energy are considered in the form of energy flux, which is defined as the amount of energy received on a horizontal snow surface of unit area over unit time. The positive value of Q_m will result in the melting of snow. The relative importance of the various heat transfer processes involved in melting of a snowpack depends on time and local conditions. For example radiation melting dominates the weather conditions when wind is calm. Melting due to sensible heat flux dominates under warm weather conditions. When all the components of energy balance equation are known, the melt rate due to energy flux can be expressed as,

$$M = Q_m / [\rho_w \cdot L \cdot \beta] \quad (2.2)$$

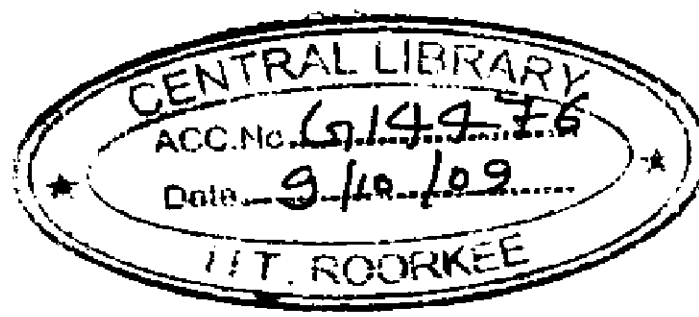
where,

M = depth of meltwater (m/day)

L = latent heat of fusion (333.5 kJ/kg)

ρ_w = density of water (1000 kg/m³)

β = thermal quality of snow



The thermal quality of snow depends on the amount of free water content (generally 3 – 5 %) and temperature of the snowpack. For a snow that is thermally ripened for melting and contains about 3% of free water content, the value of β is 0.97. For such cases equation (2.2) reduces to,

$$M = Q_m / [1000 * 333.5 * 0.97] \quad (2.3)$$

which leads to a simple relationship,

$$M = 0.0031 * Q_m (\text{mm/day}) \quad (2.4)$$

Data required to evaluate Equation (2.1) are measurements of air temperature, albedo, wind speed, vapour pressure and incoming solar radiation (Anderson, 1973). These data are difficult to obtain on a basin scale and extrapolation to areal values from point data is another problem, especially the spatial detail is required for distributed models. This becomes further difficult when such data is required for a highly rugged terrain, such as Himalayan terrain. As such application of the energy balance equation is usually limited to small, well-instrumented or experimental watersheds.

2.2.2 Degree-day approach or Temperature index approach

The specific type of data required for the energy budget method is rarely available for carrying out the snowmelt studies. This is particularly true for the Himalayan basins where the network for data collection is poor. The commonly available data in the Himalayan basins are daily maximum and minimum temperatures, humidity measurements and surface wind speed. This is why the temperature indices are widely used in the snowmelt estimation. It is generally considered to be the best index of the heat transfer processes associated with the snowmelt. Air temperature expressed in degree-days is used in snowmelt computations as an index of the complex energy balance tending to snowmelt. A 'degree-day' in a broad sense is a unit expressing the amount of heat in terms of persistence of a temperature for 24-hour period of one-degree centigrade departure from a reference temperature. The simplest and the most common expression relating daily snowmelt to the temperature index is,

$$M = D(T_i - T_b) \quad (2.5)$$

where,

M = melt produced in mm of water in a unit time

D = degree-day factor ($\text{mm } ^\circ\text{C}^{-1}\text{day}^{-1}$)

T_i = index air temperature ($^\circ\text{C}$)

T_b = base temperature (usually 0°C)

Daily mean temperature is the most commonly used index temperature for snowmelt.

The mean temperature is computed by,

$$T_i = T_{\text{mean}} = (T_{\text{max}} + T_{\text{min}}) / 2 \quad (2.6)$$

There are several methods of dealing with the index temperatures used in calculating the degree-day value. When using the maximum-minimum approach, the most common way is to use the temperature as they are recorded and calculate the average daily temperature. It was reported that sometimes the degree-days from the daily mean temperature are found to be misleading. In many parts of the Western U.S. mountainous areas, the drop in minimum temperature is so much that the daily mean temperature comes to below 0 °C, thereby indicating no possible degree-days, whereas snowmelt conditions have prevailed during a part of the day when air temperatures were much above the freezing point. The inclusion of minimum temperature at an equal weight with the maximum temperature gives undue emphasis to this effect. On the other hand the use of maximum temperature only excludes this effect entirely. In order to counteract such problems, alternatives have been suggested in which unequal weight to the maximum and minimum temperature are given. U.S. Army Corps of Engineers (1956), used the following index temperatures,

$$T_i = (2T_{\text{max}} + T_{\text{min}}) / 3 \quad (2.7)$$

Another approach is given by,

$$T_i = T_{\text{max}} + (T_{\text{min}} - T_{\text{max}}) / b \quad (2.8)$$

where,

b is a coefficient less than 2.

When the basin is subdivided based on elevation zones, the degree-days are extrapolated to an elevation zone by using a suitable lapse rate i.e.,

$$T_{ij} = \delta(h_{st} - h) \quad (2.9)$$

where,

T_{ij} = degree-day of the elevation zone

δ = temperature lapse rate in °C per 100 m

h = zonal hypsometric mean elevation in m.

h_{st} = altitude of the temperature station in m.

In a basin with little seasonal variation, a lapse rate of 0.65 °C /100 m has been found to be suitable. A study carried out by Singh (1991) indicates that a lapse rate of 0.65 °C /100 m. is suitable for Satluj basin in Himalayas.

2.3 SATELLITE REMOTE SENSING OF SNOW COVER

Distributed hydrological models, which can account for the spatial variability of basin physiography and meteorological inputs, have the potential to exploit detailed snow cover data, including distributed SCA. Conventional snow cover data, such as snow surveys, provide detailed information on such snow pack properties but their site specific nature and infrequent occurrence limit their potential for use in distributed models. In order to provide distributed information characterizing the snow cover of a watershed, snow survey measurements must be extended to regions

where no snow survey data are available. Remote sensing offers a significant potential for collecting this data in cost effective manner. Because of difficult access and expensive operation of hydrological stations, radar or satellite data are particularly appropriate. However, ground truth data are indispensable in the calibration and verification of remotely sensed data. Aerial and satellite surveys are useful in mapping snow lines. The wealth of observational material obtained by remote sensing can be integrated into models, such as snowmelt runoff models, considerably improving the forecast accuracy. Snow was first observed by satellite in eastern Canada from the TIROS-1 satellite in April 1960. Since then, the potential for operational satellite based snow cover mapping has been improved by the development of higher temporal frequency satellites such as GOES (Geostationary Operational Environmental Satellite), Landsat, SPOT and IRS series, and NOAA-AVHRR, NIMBUS-SMMR and DMSP SSM/I satellites.

Snow has a high albedo in the visible region of the electromagnetic spectrum compared to most natural surface cover. For this reason snow covered area maps were one of the first satellite remote sensing applications. The technology has developed to the point where image processing systems are widely available (Baumgartner and Rango, 1991) and percent SCA estimates on a watershed basis can be obtained in near real-time for most of North America (Carroll, 1990; NOAA, 1992).

The net radiation balance is usually the most important factor in the snow pack energy budget and snow covered area (SCA) estimates can provide a means to estimate the net radiation flux over a discontinuous snow pack. However, few hydrological models make use of SCA, partly because data are difficult to obtain. Exceptions are the U.S. National Weather Service River Forecast Simulation

(NWSRFS) model (Anderson, 1973) and the Snowmelt Runoff Model (SRM). In the NWSRFS model SDC's are used to relate basin water equivalent to basin SCA in order to apportion the energy balance and melt. The SDC's are basin dependent and are generally developed as part of calibrating the model to a particular watershed. In the SRM, the SCA is used directly in the regression-based degree-day melt equation, incorporating a procedure to update the SCA using Landsat imagery. Elevation bands are used in addition to snow cover depletion curves to account for the SCA. Both the NWSRFS and SRM models have worked particularly well in alpine watersheds, which typically have long ablation periods and snow cover depletion patterns that are similar from year to year.

The network of geostationary meteorological satellites allows mapping of both snow and ice from several high mountainous regions of the world, and allows a comparison to be made of large-scale seasonal changes. However, the spatial and spectral resolution of the sensors on board these satellites is too coarse for snow cover mapping. The high-resolution satellites, such as Landsat, SPOT, IRS and JERS and the medium resolution satellites such as NOAA are widely used for mapping snow cover (Baumgartner et al., 1986). However, the repeat cover period for high resolution satellites such as Landsat is 16 days, which is not adequate for mapping shallow snow cover that can completely melt between consecutive overpass. Also, clouds often obscure visible imagery of the earth's surface and thus estimates of watershed state parameters using visible imagery are not a reliable source of data. However, mapping of shallow snow cover would be useful if provided at the daily repeat coverage intervals of meteorological sensors such as GOES or NOAA. GOES and NOAA imagery have an approximate spatial resolution of 1 km.

Another possible source for snow cover information is microwave satellite imagery. The regular and frequent mapping of snow cover is possible using a sensor independent of time and weather. Depending on wavelength, microwave radiation will penetrate clouds and most precipitation, thus providing an all-weather observational capability, which is very significant in snow regions where clouds frequently obscure the surface. There are two types of microwave sensors: active and passive. Active satellite sensors contain synthetic aperture radar (SAR) and emit microwave radiation at a specific frequency and polarization and measure the return backscatter in the form of the backscatter coefficient. Passive radiometers include NIMBUS-7 Scanning Multi-channel Microwave Radiometer (SMMR) and the DMSP SS/I. Satellites and measure surface brightness temperatures

Microwaves have unique capabilities for snow cover modeling:

1. They can penetrate cloud cover providing reliable data;
2. They can penetrate through various snow depths depending on wavelength therefore potentially capable of determining internal snowpack properties such as snow depth and water equivalent.

Microwave sensors have been studied as potential sources for snowcover information. of interest in the studies is measurement of the snow cover areal extent, depth and water equivalent.

Active microwave sensor was there on the First European Remote Sensing Satellite (ERS-1) and Canadian RADARSAT offer the possibility to observe seasonal snow cover characteristics in detail over the entire snow-cover season. In one simulation of RADARSAT data, snow-cover classification accuracy was 80%, comparable to aircraft Synthetic Aperture Radar (SAR). Comparing a classification of snow-covered area based on SAR with that done using TM suggests that a SAR-

based classification is sufficiently accurate to substitute for visible-and-near-IR based estimates when such data are not available, for example due to cloudiness.

Passive microwave signals are also sensitive to the liquid-water content of snow, thus offering the potential to develop snow wetness estimates. The sensitivity of passive microwave signals to snow wetness aids in determining the onset of spring melt and the occurrence of multiple melt events during the winter. In passive mode, microwave emission is strongly dependent on the condition of the snow in terms of humidity, metamorphism and water equivalence. Microwave penetration depth of dry snow is much larger and dry snow cover less than 2.5 cm depth is transparent to the microwaves and ignored even though it is thick enough to reflect incoming short-wave radiation. The interaction of microwaves with snow strongly depends on the snow wetness, size and structure of snow grains. The dielectric constants of water and snow are so drastically different that even a little melting will cause a strong microwave response. It is found good agreement between aircraft and microwave depth estimates for an Alaskan snowpack; but they also noted that the radiometric correction for the effect of atmospheric absorption is important at all wavelengths used for a reliable estimation of snow depth. Experimental snow mapping with satellite derived passive microwave radiometer data show the high potential of mapping for dry. However, the poor spatial resolution of the satellite microwave sensors, typically of the order of 25km, has restricted the use of snow cover values estimated from passive remote sensing for snowmelt run-off determination in high mountainous catchments.

Several researchers have reported on efforts to incorporate remote-sensing data into snowmelt-runoff modeling. Researchers reviewed the progress that has been made for incorporating remote-sensing data into regional hydrologic models of

snowmelt runoff. The National Oceanic and Atmospheric Administration's (NOAA) Advanced Very High-Resolution Radiometer (AVHRR) sensor provides daily views over large areas (1000-km swath) and snow-cover maps are produced operationally. In large basins ($>10^3$ km²) AVHRR or other medium resolution sensors provide daily coverage in cloud free weather and are used for operational snow snow maps by the US NWS and in some applications of SRM (e.g., Baumgartner et al., 1986). Estimates of snow-covered area based on remote sensing data can significantly improve the performance of even simple snowmelt models in alpine terrain. For operational purposes, empirical approaches using combination of remote sensing data to estimate snow-covered area, and snow-depth networks to estimate SWE are continuing to improve (Martinec et al., 1991). If SCA observations can be provided at intervals of a week or two, SRM can be used for forecasting without any historical data on snow cover depletion.

2.4 SNOWMELT STUDIES FOR HIMALAYAN BASINS

The snowmelt studies carried out in the Himalayan region may be broadly categorized as studies related with regression analysis, empirical relationships and application of snow melt simulation models.

2.4.1 Development of regression relationships

In the regression analysis category, regression was carried out to co-relate the snow cover area with the runoff. Efforts were also made to co-relate the winter snowfall and snowmelt runoff. The satellite imageries were used for finding the

snow covered areas during early April over the Indus river and the Kabul river in Pakistan which was regressed with the flows of April to July for the years 1969-73. The early spring snow covered area was significantly related to April through July 31 streamflow, in regression analysis for each watershed. Predictions of the seasonal flows for 1974 using the regressed equations obtained were found to be within 7% of the actual flow. The relationship between snow cover area and runoff of the Beas basin has been studied by Gupta et al., (1982). Snow cover area was mapped from Landsat imageries and the snow cover area and the subsequent runoff in different sub-basins was found to be well co-related. It has been interpreted that there have been years of uniformly heavier and lighter snowfall all over the basin and snowmelt discharges have systematically varied.

Bagchi, (1981), estimated the snowline altitude and the snow cover using Landsat imageries for Tons river basin in Himalayas. A relationship was observed between the snowline of Beas, Ravi and Tons. Lean season discharge of Sainj river has been studied in reference to winter snowfall and discharge, to establish the relationship between two variables. The studies have revealed that both these parameters have a high co-relation coefficient of 0.91. Based on this study, a simple linear regression model was evolved to forecast (three to four months in advance), the lean season discharge of Sainj river solely on the basis of winter snowfall.

Dey and Goswami, (1983), have presented results of studies involving utilization of satellite snow cover observations for seasonal stream flow estimates in Western Himalayas. A regression model relating seasonal flow from April through July 1974 to early April snow cover, explained 73% and 82% of the variance, respectively, of measured flows in Indus and Kabul rivers. The importance of permanent snow covered area in the study of the snowmelt was brought out by

Ferguson, (1985). A study was carried out for the glacierized mountains (Upper Indus in Pakistan) and a model was developed for annual variation of runoff and its forecasting. The approach is based on identification of a number of glaciological and climatological factors other than snow covered area. The information about extent of snow cover obtained from the Landsat MSS imageries for the months of March to June with the snowmelt runoff assumed as total flow minus baseflow for different sub-basins of Chenab river was related. A general linear relationship was obtained. A study to develop a regression relationship between temperature of Kaza and snowmelt runoff collected at a proposed dam across Spiti river, about 4 km upstream of Kaza at an elevation of about 3639 m, in the Satluj basin.

A regression model using percentage of snow covered area of Satluj basin up to Bhakra dam and seasonal snowmelt runoff (April -- June) for the years 1975-78 was attempted. The model was used to forecast the seasonal snowmelt runoff in Satluj for 1980. At the end of June 1980 it was found that the difference between the forecast quantity and observed flows was about 9%.

2.4.2 Application of empirical relationships

Several snowmelt studies using empirical relationships between temperature and snowmelt runoff have been made. Such empirical relations are generally a function of degree-day factor and snow cover area. Snowmelt was estimated by considering the melt due to influence of temperature and rainfall in the snow covered area for Beas basin up to Larji. The relationship between snow cover acquired with the help of satellite imageries and the cumulative discharges of the months of March, April and May for the year 1973, 1975, 1976 and 1977 was

studied. Due to availability of limited meteorological and hydrological data, the estimation of snowmelt runoff has been limited to the sub-basin upstream of Manali.

Bagchi, (1981), carried out a study of snowmelt runoff in Beas basin using satellite images. Temperature index method was employed using a lapse rate of $0.65^{\circ}\text{C}/100\text{m}$. The value of degree-day factor was considered as $2.1 \text{ mm } ^{\circ}\text{C}^{-1}\text{day}^{-1}$. The study was carried for the Beas basin up to Manali. An empirical model for prediction of snowmelt runoff in Satluj basin has been used by Upadhyay et al., (1983). The model for computation of snowmelt runoff has been presented as a function of degree-day factor. Upadhyay et al., (1983), also analyzed the various components of energy input to a snow cover and monthly budget for net energy available for snowmelt have been worked out for a number of stations in Himalayas.

The snowmelt runoff generation for a sub-catchment of Beas basin was made using point energy and mass balance approach. The contribution of various energy sources in different conditions was also worked out. Snowmelt runoff was estimated using the degree-day method. Snowmelt thus arrived was compared with the observed discharge. The study was based on the data for the year 1981-92 collected from the snow courses located in the sub-catchment. Results indicate that although net radiation balance remains the dominant source of melt energy, yet sensible and latent heat contribute in the range of 40% to 60% of the total energy for the altitudes below 3000 m in the open area during clear and partly cloudy days in the active snowmelt period. The influence of radiation on cloudy days ranges from 20% to 34%. Upadhyay et al., (1985), have shown that for Beas and Satluj basin, the snowmelt caused by the incoming solar radiation is predominant over other physical processes such as long wave energy transfer at the snow-air interface, convective heat exchange and latent heat released by condensation. It was shown that the

results obtained by the degree-day approach varied significantly from the results obtained by energy balance approach.

2.4.3 Application of simulation models

Only limited studies have been carried out either to develop or to test the existing models for simulation of snowmelt runoff in the Himalayas. A snow melt runoff model was developed and verified using 1977, 1978 and 1979 data of Beas river basin up to Manali. The model uses the information regarding the aerial extent of permanent and temporary snow cover obtained through satellite imageries, observed data of precipitation for November to May and daily temperature for the pre-monsoon season. The model considers the altitudinal effect on temperatures, the orographic effect on precipitation, meltwater effect of rain falling on the snow-covered area. Simple routing relation was used for obtaining the daily stream flow at the catchment outlet. It was found that the results generally improved by increasing the number of elevation zones. Singh, (1989), tested the snowmelt runoff model for Beas basin up to Manali for a limited period. The results of the model were found satisfactory with a goodness of fit as 0.83 and 0.61 for the years 1978 and 1979 respectively. Dey et al., (1989) employed the SRM to simulate runoff during the snowmelt season from the Kabul river basin in the Himalayas. Several potential modifications were carried out to account for certain factors that give poor simulation due to location of climate stations being vertically and horizontally at a great distance from the snowmelt contributing area, unrepresentative lapse rates etc. These modifications improved the simulation accuracy, quite significantly.

SRM model was applied for two study areas viz. The Beas basin up to Thalot and Parbati River up to Pulga dam site. Landsat MSS data for the runoff seasons of 1986 and 1987 were digitally analysed using sophisticated interpretation techniques. The areal extent of the snow cover was evaluated for each elevation zone. This information along with data regarding temperature, precipitation, degree-day factor, temperature lapse rate and runoff coefficients were input into the model, which runs on a personal computer. Simulation studies were carried out to obtain a good fit between the simulated discharges at Thalot and Phulga dam site, and the actual discharges as measured by user departments.

THE STUDY AREA AND DATA USED

CHAPTER 3

3.1 THE STUDY AREA

In this study, Chenab River up to Premnagar has been selected and location of the same is shown in Figure 3.1 and drainage map of the study area is shown in Figure 3.2. The Chenab River is one of the five main rivers of the great Indus System. The major part of the Chenab catchment lies in India; its lower reach including the confluence with the Indus River is in Pakistan. It spreads over the two states of India, namely, Himachal Pradesh and Jammu & Kashmir which comprise the extreme western sector of Himalayas. Upper half of this basin is located between the Zaskar and the Pir-Panjal ranges whereas the lower half is located between the Pir-Panjal and the Dhauladhar ranges. In this way, this basin covers outer, middle and greater Himalayas.

The Chandra and the Bhaga rivers join together to form the Chandrabhaga or the Chenab. The Chandra starts from a large snowbed on the south-eastern side of Baralacha Pass at an elevation of 5,639 m and after flowing (south-east) through snow clad barren area for about 90 km, it sweeps round the basin of mid Himalayas and joins the Bhaga at Tandi after a course of about 185 km. The combined stream, known as the Chenab, flows in north-west direction through the Pangi valley of Himachal Pradesh and enters Kishtwar area in Jammu & Kashmir. It receives its major tributary, the Marusudar River and then flows in southern direction for about 25 km. Thereafter, it flows almost in westerly direction up to the Salal Dam site. From this place, the river takes a southerly

turn and emerges out into plains near Akhnoor. A little further, the river enters in Pakistan. The total length of the Chenab River up to Premnagar is about 473 km and the catchment area is 16963 km².

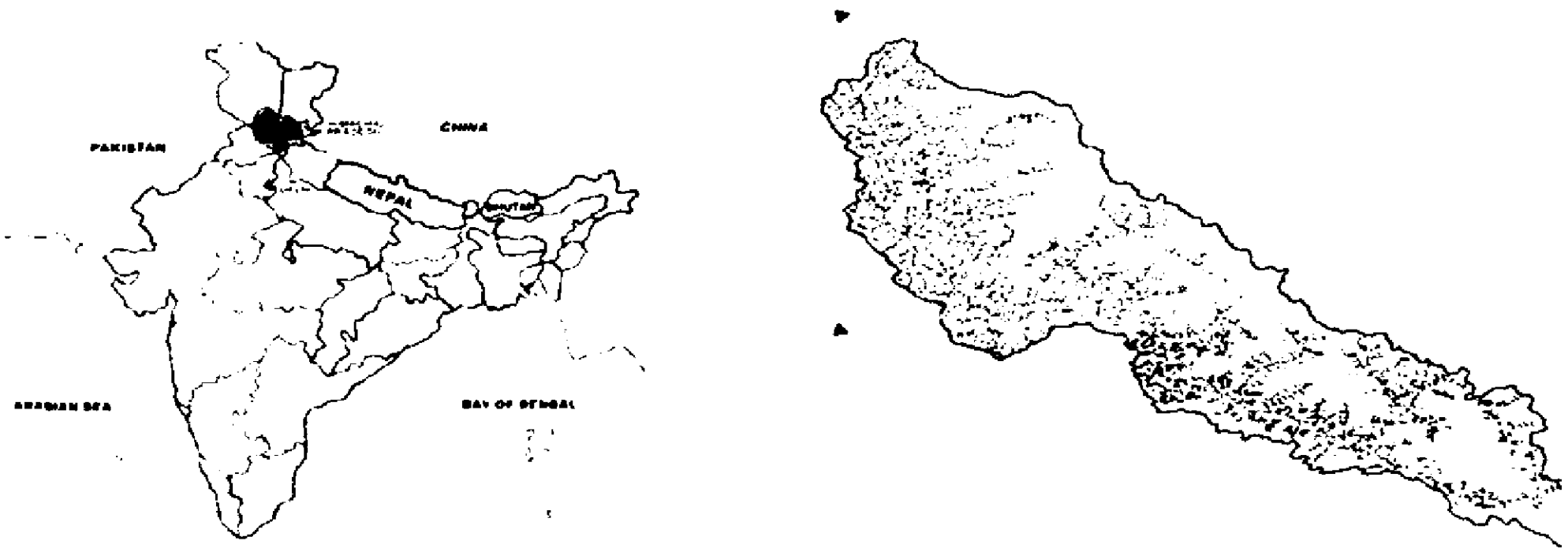


Figure 3.1 Location map of the study area

3.2 DATA USED

3.2.1 Topographic data

The Chenab basin up to Premnagar in India falls in toposheet nos. 43 N,O,P and 52 B,C,D,F,G,H at a scale of 1:250,000.

3.2.2 Hydrometeorological data

In the Chenab basin, up to Premnagar, rain is observed at 9 locations. Data has been collected from 1999 to 2007. The location of raingauge in Chenab basin is

shown in Figure 3.3. In the present study, raingauge data of Darabsala, Sirshi, Bhadarwah, Hawal, Mau, Tandi and Koksar have been used.

To monitor the river flows, there are 10 discharges sites. Data has been collected from 1989-90 to 2006-07.

There is not temperature data. Therefore temperature data of neighboring catchment i.e. Beas basin have been used. The temperature considered at the same altitude for which it was available.

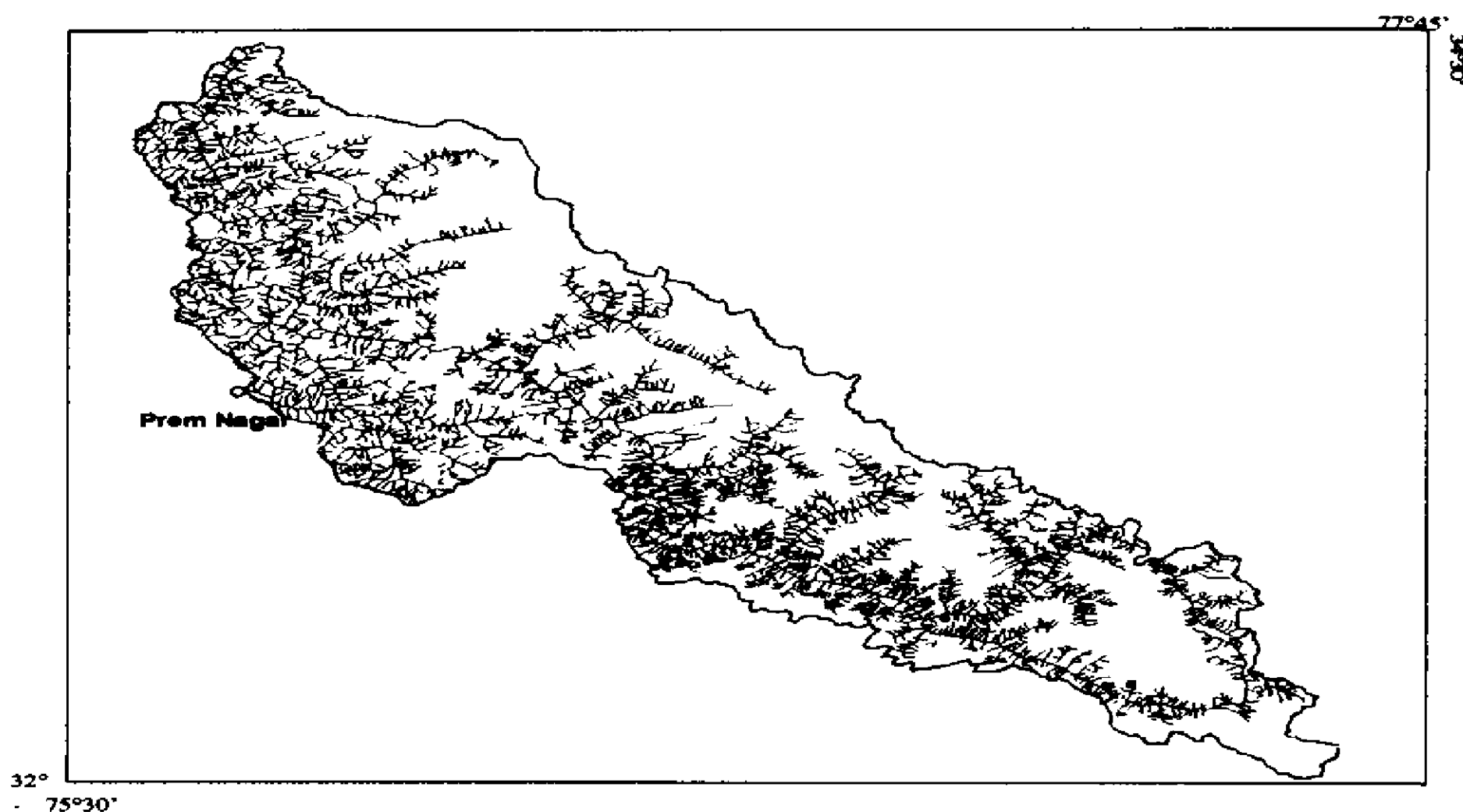


Figure 3.2: Drainage map of the study area

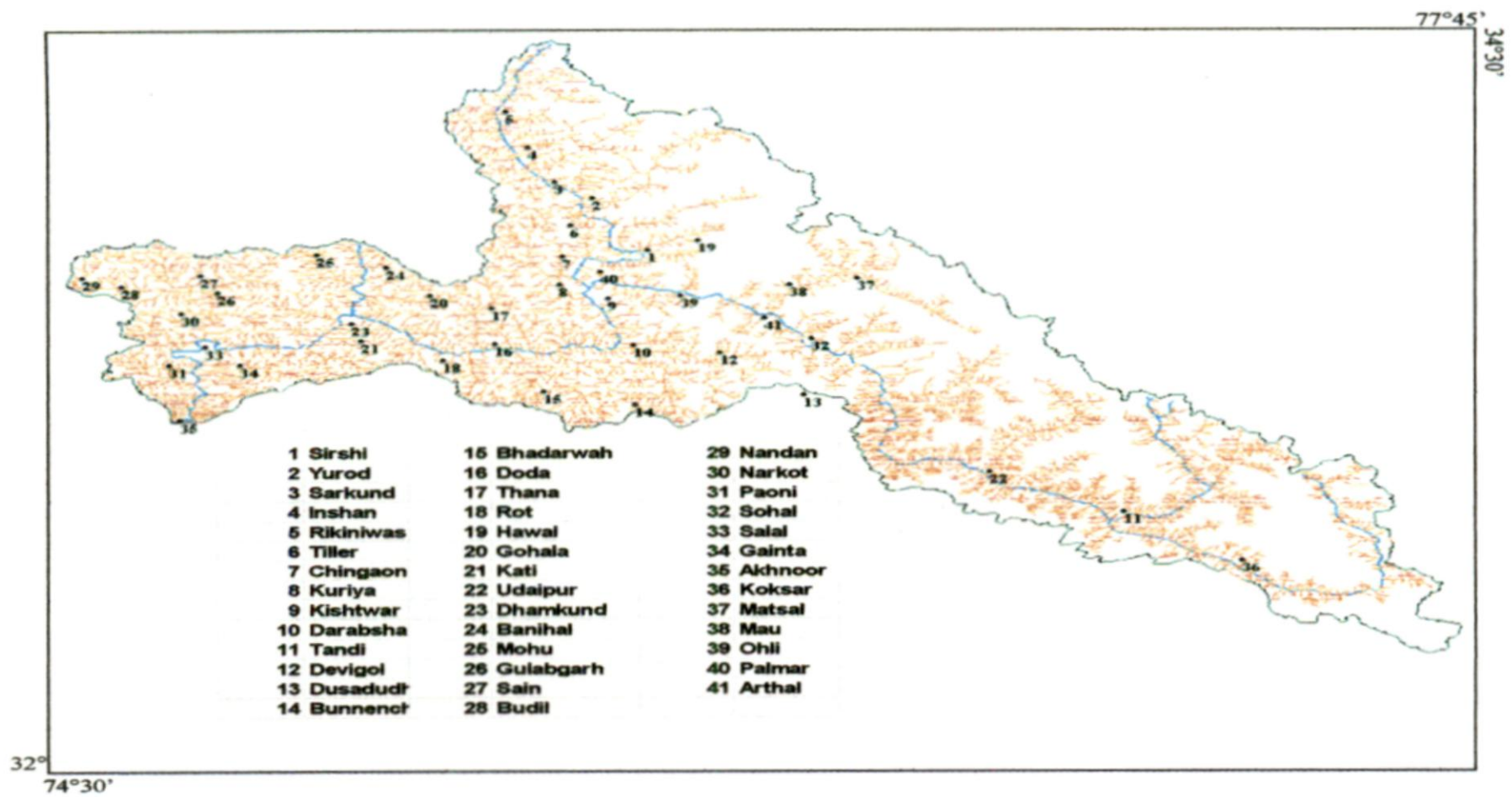


Figure 3.3: Chenab basin with raingauge locations

3.2.3 Remote sensing data

In this study, MODIS data have been used for preparation of snow cover maps and for topography, SRTM DEM has been used. The maximum and minimum (permanent) snow covered areas are determined using remote sensing data (MODIS) for all the months .

The description of both the data sets is given in the following sections.

3.2.3.1 MODIS Data

The Moderate Resolution Imaging Spectroradiometer (MODIS), flown on board the Terra Earth Observing System (EOS) platform launched in December 1999, produces

a snow-covered area (SCA) product. This product is expected to be of better quality than SCA products based on operational satellites (notably GOES and AVHRR), due both to improved spectral resolution and higher spatial resolution of the MODIS instrument.

MODIS is an environmental satellite operating in visible, near and short wave infrared and thermal portions of the electromagnetic spectrum and acquires image in 36 spectral bands. It has spatial resolution of 250, 500 and 1000 m depending on the spectral band and has a swath width of 2330 km enabling to view the entire surface of the earth every 2 days. MODIS image have a potential to provide quantitative measures of numerous geophysical parameters including snow cover.

The MODIS snow-mapping algorithm utilizes seven MODIS bands designed especially to image the land surface. This algorithm is a fully automated and computationally frugal approach to snow detection. It is based on a series of tests for snow detection including Normalized Difference Snow Index (NDSI) and other criteria tests. Currently, a suite of snow cover products is being produced from MODIS data and is distributed by the Distributed Active Archive Center (DAAC) located at the National Snow and Ice Data Center (NSIDC). The snow product is the MODIS/Terra Snow Cover 5-Min L2 Swath 500 m (MOD10_L2) product. It is so named because it represents snow cover acquired in approximately 5 min of MODIS scans. It has a nominal spatial resolution of 500 m and a swath width of 1354 km across track and 2030 km along track length. MOD10A1 data product is the spatial composite of individual snow observations from all daily MOD10_L2 products covering a particular area (Klein et al., 2003). A set of five MODIS snow cover products is currently being distributed to the user community through the NSIDC DAAC (<http://LPDAAC.usgs.gov/dataproducts.asp>). This suite of

snow products represents a progression of products ranging from snow cover maps produced from individual MODIS swaths (scenes) to spatial and temporal composites covering 8-day periods at spatial resolutions of 0.05×0.05 degree. The MODIS Snow Products Users' Guide contains detailed information pertaining to the structure of and information contained in all MODIS snow products (Riggs et al., 2003). The summary of MOD10A1 data is listed in Table 3.1.

Table 3.1: Summary of the MOD10A1 product

Earth science data type (ESDT)	Product level	Nominal data array dimensions	Spatial resolution	Temporal resolution	Map projection
MOD10A1	L3	1200km * 1200km	500m	daily	GCTP Sinusoidal

(Source Riggs et al. 2003).

3.2.3.2 SRTM 90m Digital Elevation Data

On February 19, 2000, the space shuttle carried onboard, for the first time, a space borne, single-pass interferometer. The mission was referred to as the Shuttle Radar Topographic Mission (SRTM). SRTM successfully mapped the topographic features of Earth's landmasses using radar interferometry (Leblanc et al., 2006). A radar interferogram is produced by measuring the radar phase difference between two spatially separated antennas, A1 and A2 (Zebker et al., 1994). The near global coverage DEM was

produced from the C-band data and processed by NASA's JPL and the X-band data provided slightly higher resolution and were processed by the German space agency's aerospace center (DLR). This method requires no ground control, and hence is very useful for inaccessible regions. The overall absolute horizontal and vertical accuracy of these 1 arc second data is estimated to be significantly better than the original mission requirements of 20 m and 16 m respectively (Rosen et al., 2001; Sun et al., 2003). The spatial resolution of the SRTM DEM is 3-arc sec (approximately 90 m). Vertical reference of the SRTM DEMs is the WGS84 EGM96 geoid. This data is currently distributed free of charge by USGS and is available for download from the National Map Seamless Data Distribution System, or the USGS ftp site (<http://edcsns17.cr.usgs.gov/srtm/index.html>). The DEM files have been mosaiced into a seamless global coverage, and are available for download as 5° x 5° tiles, in geographic coordinate system - WGS84 datum. These files are available for download in both Arc-Info ASCII format, and as GeoTiff, for easy use in most GIS and Remote Sensing software applications. The DEM of the study area is shown in Figure 3.4.

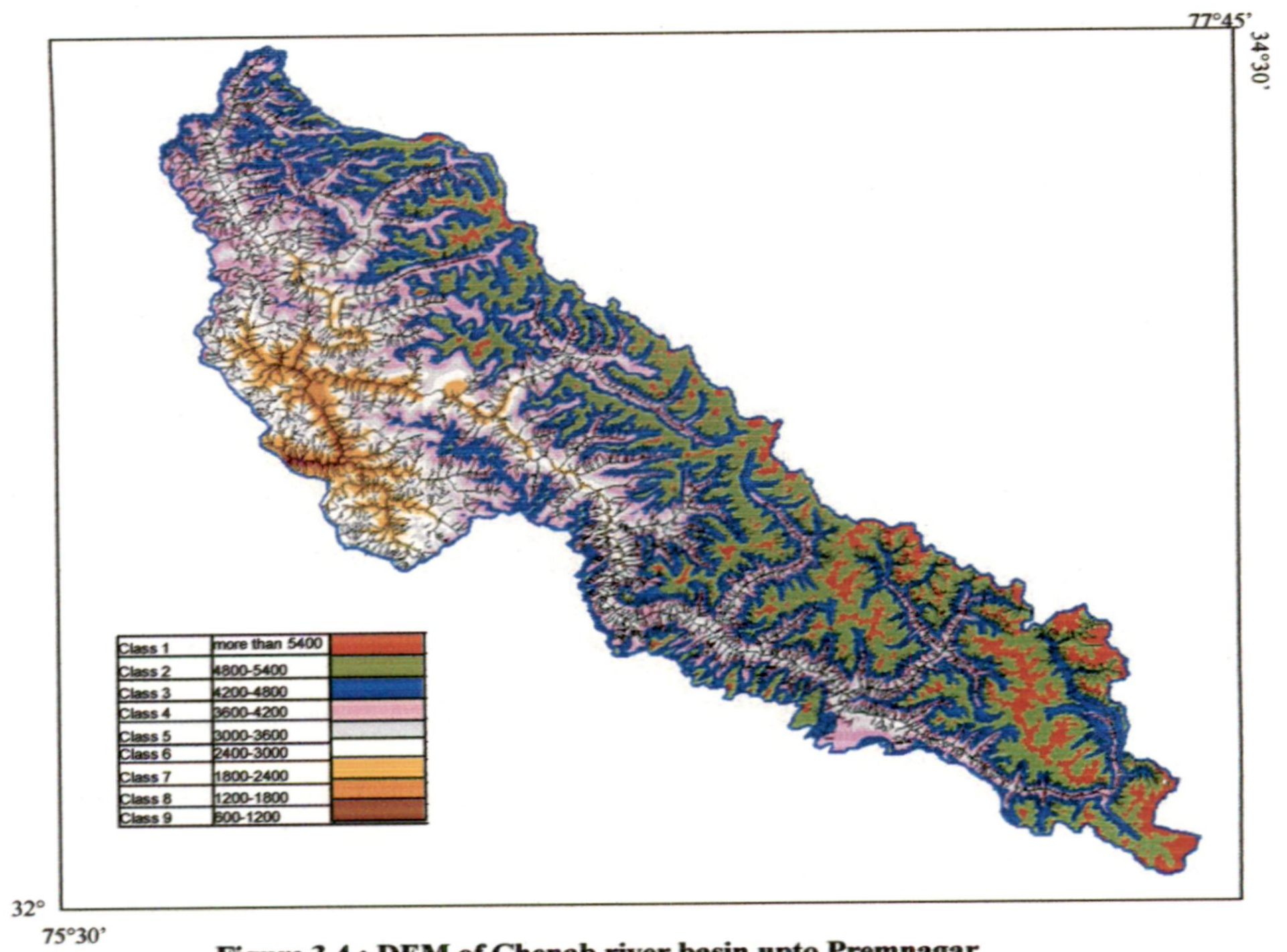


Figure 3.4 : DEM of Chenab river basin upto Premnagar

4.1 SNOWMELT RUNOFF MODELING

In most part of the world the seasonal short-term variation in streamflow reflects the variation in rainfall. But in higher latitude and altitudes where snowfall is predominant, runoff depends on heat supplied for snowmelt rather than the timing of precipitation. Hence, to understand the hydrological behavior and simulate the streamflow it is very important to model the snowmelt runoff. One of the objectives of this study is to simulate the snowmelt runoff in Chenab basin.

In the last few decades a wide range of hydrological models were proposed for different application from purely statistical methods which neglects the physics of snowmelt process to the complicated energy budget equations. But the most popular among them are the conceptual models, which represent a compromise between scientifically realistic complexity and practically realistic simplicity because of the difficulties in obtaining input data varying in time and space (Sorman, 2005).

The conversion of snow and ice into water is called snowmelt, which needs input of energy (heat). Hence the process of snowmelt is linked to the flow and storage of energy into and through the snowpack (USACE, 1998). The data required to run an energy balance model for snowmelt runoff estimation needs information on air temperature, albedo, solar radiation, wind speed and vapour pressure. The main difficulties faced are to obtain such data in basin scale and extrapolate the point data in

areal values. Another difficulty is to obtain such data for highly rugged terrain like Himalaya. Hence application of energy balance equation is limited to small and well-networked watersheds.

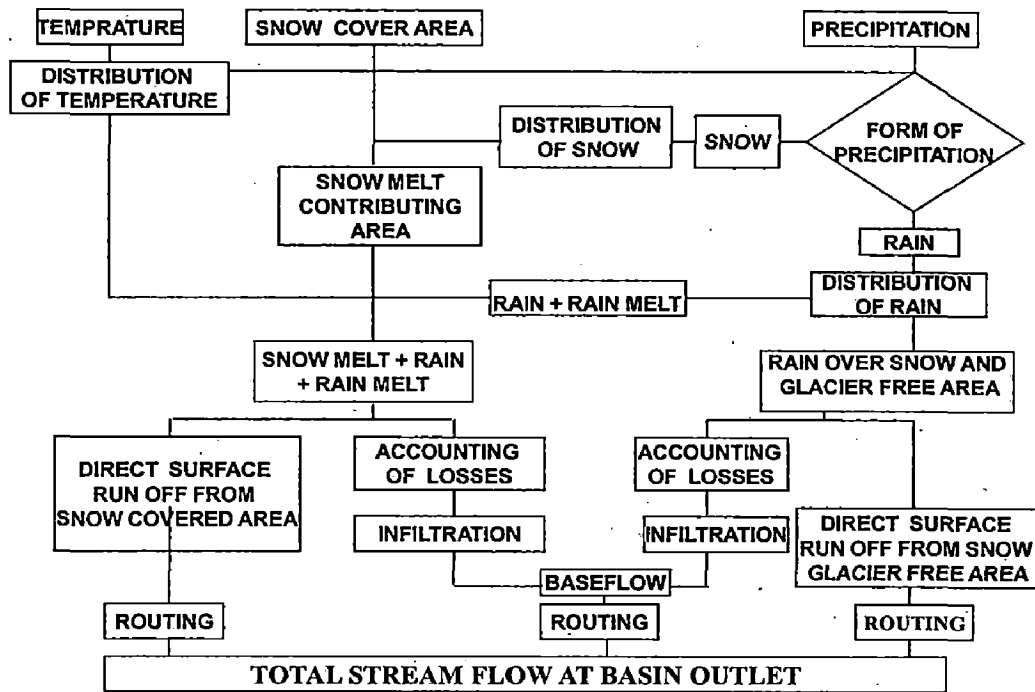
The conceptual model fully employs the concept of an “index,” where a known variable is used to explain a phenomenon in a statistical rather than in a physical sense. The most commonly available data for any basin is air temperature and it is considered the best index of heat transfer processes associated with snowmelt. This is why temperature indices are most widely used in snowmelt estimation. There are several temperature index based snowmelt models like SNOWMOD, the SSARR Model, the HEC-1 and HEC-1F Models, the NWSRFS Model, the PRMS Model, the SRM, the GAWSER Model. The SRM model is widely used for snowmelt modeling in Himalayan basin. The snowmelt runoff model uses snow-covered area as input instead of snowfall data, but it does not simulate the baseflow component of runoff. In other words, SRM does not consider the contribution to the groundwater reservoir from snowmelt or rainfall, nor its delayed contribution to the streamflow in the form of baseflow, which can be an important component of runoff in the Himalayan rivers, and plays an important role in making these rivers perennial. Almost all the streamflow during winter, when no rainfall or snowmelt occurs, is generated from the baseflow (Singh and Jain, 2003). The SNOWMOD model (Jain, 2001) is unique in this aspect as it simulates all components of runoff, i.e. snowmelt runoff, rainfall-induced runoff and baseflow, using limited data.

4.2 SNOWMELT MODEL (SNOWMOD)

The snowmelt model (SNOWMOD) has been developed at NIH for a Himalayan basin. (Jain, 2001), ^{Singh and Jain (2003).} The SNOWMOD is a temperature index model, which is designed to simulate daily streamflow for mountainous basins having contribution from both snowmelt and rainfall. The generation of streamflow from such basins involves with the determination of the input derived from snowmelt and rain, and its transformation into runoff. It is a distributed model and for simulating the streamflow, the basin is divided into a number of elevation zones and various hydrological processes relevant to snowmelt and rainfall runoff are evaluated for each zone.

The model performs three operations at each time steps. At first the available meteorological data are extrapolated at different altitude zones. Then the rates of snowmelt is calculated at each time steps. Finally, the snowmelt runoff from Snow Cover Area (SCA) and rainfall runoff from snow-free area (SFA) are integrated, and these components are routed separately with proper accounting of baseflow to the outlet of the basin.

The model optimizes the parameters used in routing of the snowmelt runoff and rainfall runoff. In this model seasonal lapse rate of air temperature as estimated by the technique discussed in section 4.3 is used. Figure 4.1 schematically shows the different steps involved with in the model. Besides, SCA estimated from MODIS snow product is used in snowmelt modeling.



STRUCTURE OF THE SNOWMELT MODEL (SNOWMOD)

Figure 4.1: Steps involved in SNOWMELT model

Details of computation of melt runoff and generation of streamflow from the basin are discussed below:

4.2.1 Input Data

In order to execute this SNOWMOD model, the following input data are required:

- Physical features of the basin, which include snow covered area, elevation bands and their areas, altitude of meteorological stations, and other watershed characteristics affecting runoff.
- Time variable data include precipitation, air temperatures, snow-covered area, streamflow data, and other parameters determining the distribution of temperature and precipitation.

- Information on the initial soil moisture status of the basin
- Miscellaneous job control and time control data, which specify such items as total computation period, routing intervals etc.

In application of SNOWMOD model, two important inputs are snow covered area and temperature lapse rate. In this study, these two inputs have been prepared using remote sensing data and the methodology is described in the following sections. After this, other inputs parameters/variables have been described.

4.3 SNOW COVERED AREA

Snow-covered area (SCA) has long been recognized as an important hydrologic variable for streamflow prediction (e.g. Martinec, 1975; Hall and Martinec, 1985). The presence of snow in a basin strongly affects moisture that is stored at the surface and is available for future runoff. For hydrological applications, SCA estimates are of primary importance where winter snow accumulation substantially affects spring runoff. Currently, a suite of satellite snow cover products is available through the National Snow and Ice Data Center (NSIDC). These include global daily and 8-day composite products at a spatial resolution of 500m derived from the Moderate Resolution Imaging Spectroradiometer (MODIS) instrument imagery. The MODIS snow-mapping algorithms are automated, which means that a consistent data set may be generated for long term climate studies that require snow-cover information (Hall et al., 2002). For climate and hydrological studies, the accuracy to which these products represent the actual snow

cover is critically important as it is the main determinant of their usefulness. Several studies have been conducted to evaluate the accuracy of MODIS snow products, either based on comparisons with other satellite-derived products or based on comparisons with point ground based (in situ) snow depth measurements.

Bitner et al. (2002) quantified the differences between the snow products of the National Operational Hydrologic Remote Sensing Center (NOHRSC), the National Environmental Satellite Data and Information Service (NESDIS) and MODIS for a few days in 2001. They compared the snow cover products with daily surface snow depth observations at almost 2000 meteorological stations across Canada and found that the MODIS and NOAA products have similar levels of agreement with ground data, ranging from accuracies of 80% to almost 100% on a monthly basis. The lowest accuracies were found for the snowmelt periods in forested areas. Tekeli et al. (2005) validated the MODIS snow cover maps against ground-based snow courses in and around the upper Euphrates River in Turkey, using data from the 2002/03 and 2003/04 winter seasons. The accuracy obtained by comparing synchronous MODIS and ground data was 62% and increased to 82% when allowing for a 2 day time shift. Cloud cover was considered to be the main reason for the relatively low classification accuracies. Recently, Zhou et al. (2005) statistically evaluated two MODIS snow products: the daily and 8-day composite images, for a period from February 2000 to June 2004, using streamflow and SNOTEL measurements as constraints. The inter-comparison of these two products over the Upper Rio Grande River Basin indicated that the MODIS 8-day product has higher classification accuracies for both snow and land, but slightly higher errors of misclassifying land as snow than the MODIS daily product. They concluded that for clear days, the MODIS

daily algorithm works as well or better than the MODIS 8-day algorithm. As is clear from this review, most of the validation studies used short periods of MODIS data and were carried out in North America. A lack of such studies for the Himalayan basin was the motivation for us to take up a study in a typical Himalayan basin having snow cover.

4.3.1 Methodology

The methodology followed in this study consisted of preparing the DEM of the study area, preparing snow cover map and then preparing snow depletion curves. Details of the methodology follow:

4.3.1.1 Preparation of Snow Cover Map

Terra MODIS snow cover maps are used as inputs for mapping seasonal snow cover. Terra MODIS snow cover daily L3 global 500 m Grid (MOD10A1) data from March to September between 2000 and 2005 were acquired.

The Normalized Difference Snow Index (NDSI) uses the spectral characteristics of snow and is based on the concept of Normalized Difference Vegetation Index (NDVI) used in vegetation mapping from remote sensing data (Dozier, 1989; Hall et al., 1995, Gupta et al., 2005). The NDSI is defined as the difference of reflectance observed in a visible band and the short-wave infrared band divided by the sum of the two reflectance (Gupta et al., 2005). It can be computed by:

$$\text{NDSI} = \frac{\text{Visible Band} - \text{SWIR Band}}{\text{Visible Band} + \text{SWIR Band}}$$

The MODIS snow cover product is a classified image. The pixel values of the MOD10A1 data in the study area include 1 (No decision), 25 (snow free land), 50 (Cloud obscured), 200 (Snow) and 254 (Detector saturated) (Riggs et al., 2006; Hall and Riggs, 2007). The surface land cover on pixels denoted 'No decision' and Detector saturated can not be determined, so these pixels are with those of 'Cloud obscured'. Thus, the surface land cover of snow cover maps are recoded into three classes in this study: snow, cloud-obscured land and snow-free land. According to the statistics in the study area, the percentages of 'No decision' pixels or 'Detector saturated' pixels on most snow maps are less than 1%. Therefore, the impact of these two kinds of pixels on seasonal snow cover mapping will be limited in this study. Using the classified snow maps, the total percentage of snow cover in the study area was estimated for different dates.

Using the Indian tile of the global SRTM-DEM, the DEM of the study area was extracted. It was in geographic coordinate system and WGS 84 datum plane. MOD10A1 data products were registered by taking the DEM as the master image and rest of the images as slave images. More than 30 ground control points were selected for each image in such a way that they were well spread throughout the study area to achieve higher accuracy in geo-referencing. The 2nd order transformation and nearest neighbour re-sampling technique was adopted. The root mean square error was within a pixel size. One set of SRTM DEM was re-sampled to 500 m pixel size to match with the MODIS data.

4.3.1.2 Depletion Curves

In the present study, the SCA was computed for different elevation zones. For this purpose, DEM and SCA maps were processed for all the dates. The basin was divided into 9 elevation bands with an altitude difference of 600 m for convenience. These bands

are >5400 m, 4800-5400 m, 4200-4800 m, 3600-4200 m, 3000-3600 m, 2400-3000 m, 1800-2400 m, 1200-1800 m, and 600-1200 m. These 9 elevation zones are called as band 1, band 2, band 9. The SCA in each elevation bands were plotted against the elapsed time to construct the depletion curves for all the various elevation bands in the basin for all the years. The snow cover depletion curves vary significantly from year to year and hence separate curves have been drawn for each year under consideration. In order to simulate runoff on daily scale from the basin, daily SCA for each band was used as input to the model.

The analyses for each band were carried out. It was observed that the SCA in bands 1 remains 100% throughout the year while bands 7, 8 and 9 remain snow-free throughout the years. Melting of snow starts from the month of March and there is reduction in snow cover in band 4 to 8 from March onwards till September. Therefore, mainly there is variation in the bands 4, 5, 6, 7 and 8. Band 8 is almost snow free in the months of April to September.

4.4 TEMPERATURE LAPSE RATE

In various snowmelt runoff studies, temperature lapse rate (TLR) is one of the important variables. It is defined as the rate of change of temperature with elevation. Several studies conducted in past using air temperature and station height has shown that temperature changes linearly with change in elevation (Singh, 1991; Aber and Federer, 1992). Temperature is considered to be a relatively straightforward meteorological variable to extrapolate or interpolate on climatic time scales, because temperature fields

are continuous and horizontal temperature gradients are typically low for long-term climatology, in which the effects of weather systems and fronts average out. Vertical temperature gradients are much higher, and the common practice when extrapolating temperature fields to higher or lower elevations is to assume a constant atmospheric lapse rate.

The main problem faced for calculation of TLR is limited numbers of ground stations spread in the studies area, which is not representative for the whole terrain. Especially in the case of hilly terrain like Himalaya, where climate is very sensitive to the ruggedness of the terrain, limited number of ground stations possesses a challenge to the TLR estimation.

Hence, a truly representative TLR is difficult to estimate. Due to this, in several past studies a fixed TLR value ($0.65^{\circ}\text{C}/100\text{ m}$) was used for Himalayan condition. In reality, TLR varies with season and region. A study of deScally (1997) from Punjab Himalaya, Pakistan suggests that the lapse rate in this region is generally higher than the values reported from other studies which range from 0.48 to 0.78°C per 100m . Researchers have used wide ranging lapse rate ranging from 0.65 to 0.98°C per 100 m for runoff modeling studies (Bagchi, 1982, Dey et al., 1989, Upadhyay, 1995). Many other snowmelt runoff models from various regions used range of values close to the environmental lapse rate ranging from 0.55 to 0.65°C per 100m (Martinec, 1975, Kayastha et al., 1999).

To overcome the difficulty of sparse network of air temperature, use of land surface temperature (LST) is an alternative. The temperature lapse rate estimation using

LST can be used in snowmelt runoff studies. LST data derived from satellite data are continuous datasets with better spatial and temporal resolution. It combines the results of surface-atmosphere interactions and energy fluxes between the atmosphere and the ground (Sellers et al., 1988). LST estimated from satellite data are the energy received in thermal sensors (10.5 -12.5 μm) wavelength region emitted by the land surface. It depends on latitude of the location and surface properties, specifically surface albedo and specific heat of the surface. The satellite sensor measures the infrared radiance leaving the top of the atmosphere towards the satellite; this radiance is corrected with respect to the influence of a clear (i.e. nearly non-scattering) atmosphere, the resulting radiance is converted to a temperature according to Planck's law and it is called Land Surface Temperature. The thermal infrared signature received by satellite sensors is determined by surface temperature, surface emissivity / reflectivity, and atmospheric emission, absorption and scattering actions upon thermal radiation from the surface, and the solar radiation in daytime.

The difference between air temperature and LST varies particularly with the surface water status, the roughness length and the wind speed. However, the seasonal trend of the two variables is correlated. Kawashima et al. (2000) observed that the two variables have a good correlation coefficient with standard error of 1.4 to 1.8 °C. In the central Arctic, the climatological mean difference between air temperature and the surface temperature for all skies is within 1.5 °K, varying from -0.2 °K in September and June to 1.5 °K in February, and averages approximately 0.5 °K during winter (Key et al., 1994).

4.4.1 LST Map generation from NOAA-AVHRR Images

LST is a key parameter in snowmelt runoff studies. It is generally defined as the skin temperature of the ground. For the bare soil, LST is the soil surface temperature and for snow surface, it is snow surface temperature. Satellite remote sensing provides an alternative to map this parameter in large scale. Many efforts were made to retrieve this information from satellite data. These methods are based on variety of split window algorithm developed to retrieve LST from National Oceanic and Atmospheric Administration / Advanced Very High Resolution Radiometer (NOAA-AVHRR), Geostationary Operational Environmental Satellite (GOES) or Meteosat systems.

The theoretical basis for the remote sensing of LST is that the total radiative energy emitted by a ground surface increases rapidly with temperature. The spectral distribution of the energy emitted by a ground object also varies with temperature. The thermal energy in relation to the physical temperature of the ground surface can be remotely observed by using sensors operating at the atmospheric window in the thermal infrared area of the electromagnetic spectrum (8-12 μm). The obtained temperature of the ground surface on the satellite level is called the brightness temperature.

Ever since the remotely sensed data in thermal band data became available, several approaches have been developed to determine the land surface temperature using this data. In this effort the first problem to be solved is to translate the satellite radiance into surface brightness temperature. To retrieve brightness temperature, the thermal channels have to be calibrated. The detailed procedure for calibration of the NOAA-AVHRR thermal channels is available at <http://www2.ncdc.noaa.gov/docs/podug>.

Brightness temperature can be obtained from the thermal bands of channels 4 and 5 of NOAA-AVHRR images using inverse Planck's equation. Starting from NOAA-15 satellites, NESDIS (National Environmental Satellite, Data and Information Service) incorporates the non-linear radiance corrections for AVHRR thermal channels 4 and 5. Hence, the radiance measured by the sensor (E_i) was computed as a non-linear function of the input data values as follows (NCDC, 2003):

$$E_i = A_0 + A_1 C_i + A_2 C_i^2 \quad (4.1)$$

Where, A_0 , A_1 , and A_2 , (for channels 4 and 5) are constants and C_i is the input data value (Digital Number) for channels 4 and 5 ($i = 4, 5$).

Following the Planck's equation, for the central wavelength V_{Ci} for channels 4 and 5, an effective brightness temperature (T_{Ei}^*) was calculated for each channel. Finally, the brightness temperature for each Channel was calculated using the (T_{Ei}^*) as follows:

$$T_{Ei} = B_0 + B_1 T_{Ei}^* \quad (4.2)$$

The values of B_0 and B_1 (for channels 4 and 5) are constant and can be found in NOAA-KLM header of the HRPT (or Level 1b) images. The value of the central wave number of each channel can be also found there, as well as the satellite height (and other parameters) that are needed to correct AVHRR panoramic distortion.

These brightness temperatures are then converted to LST using split-window method. Many studies were conducted to retrieve LST using thermal infrared radiation emitted from the surfaces using split-window algorithm (Becker and Li, 1990; Coll and

Caselles, 1997; Sobrino and Raissouni, 2000). The split-window algorithm uses two adjacent thermal infrared channels, centered at 11 μm and 12 μm , for AVHRR to retrieve surface temperatures because of their different atmospheric transmittances. The split window LST method corrects the atmospheric effects based on the differential absorption in infrared bands. The accuracy of the split-window algorithm depends on the magnitude of difference between the emissivities of the surface in the two bands. The general form of the split-window equation can be written as

$$T_s = T_4 + A(T_4 - T_5) + B \quad (4.3)$$

Where, T_s represents the land surface temperature, A and B are the coefficients determined by the impact of atmospheric conditions and other related factors on the thermal spectral radiance and its transmission in channels 4 and 5. T_4 and T_5 are the brightness temperatures in channels 4 and 5 respectively. Apart from the general form of the equation 3, different authors have proposed other forms of the split window algorithm for the retrieval of LST from AVHRR data (Vogt 1996).

4.4.2 Temperature Lapse Rate Estimation

As discussed earlier, the visual inspection of LST map and DEM clearly shows that the temperature follows similar pattern as elevation. To better understand the mathematical relation between the LST (dependent variable) and elevation (independent variable), regression analysis was performed.

In this study, NOAA LST and MODIS LST maps were extracted from the MOD11A1 and MOD11A2 data products. Using this LST map and SRTM DEM, TLR was determined for different periods during the years 2000 to 2005.

The first step involved was to plot the two variables in two dimensions as a scatter plot. The scatter plot allows us to visually inspect the data prior to running a regression analysis. The graphs were drawn between LST values obtained from MODIS datasets and air temperature. The scatter plots clearly show that temperature decreases with increase in elevation in a linear manner. The equations of the regression line or the best-fit line were obtained using least square method. The equation of the best-fit line or the regression equation can be generalized as follows:

$$Y = -aX + b \quad (4.4)$$

Where,

‘X’ are the elevation values and ‘Y’ are the temperature values. The coefficient – ‘a’ is the slope of the straight line.

Since, the slope of the line is negative; it indicates that the temperature and LST values are inversely related to each other. The values of coefficient of determination (R^2) were also computed for the scatter plots. R^2 represents the fraction of initial variance accounted for the relationship and it varies between zero and one. If the value is zero then it indicates that the two variables are not related to each other. In the present study, R^2 values between 0.62 and 0.80 were obtained in case of LST estimation from MODIS-LST maps, which indicates that the model is working reasonably well.

4.5 MODEL VARIABLES AND PARAMETERS

4.5.1 Division of catchment into elevation bands

There are two approaches for defining a computer model of a watershed; a lumped model, which does not take into account spatial variability of processes, and a distributed model, which consider these. Lumped model is a simple approach and can be applied for basins that have a wide variety of physical features. However, the major limitation with this model is that it does not run beyond a single event (USACE, 1998). Distributed model on the other hand can be run for continuous simulation. In such models, the watershed is divided into subunits with variables being computed separately for each. This method of subdividing the basin is logical one, since in mountainous areas hydrological and meteorological conditions are typically related to elevation.

SNOWMOD is a distributed hydrological model, which allows the basin to be divided into number of bands. The number depends upon the topographic relief of the basin. There is no specified range of altitude for slicing the basin in the bands, but an altitude difference of about 500 to 600 m is considered appropriate for dividing the basin into elevation bands. Moisture input for each band is the sum of snowmelt and rainfall. Runoff for each band is computed from watershed runoff characteristics developed for that particular band. Streamflow for the whole basin is obtained by summing the runoff synthesized for all elevation bands. The program stores a value for each component of flow and each routing increment for every elevation band. It maintains an inventory of snow cover area, soil moisture, snow accumulation, and all other values required for making the computation for the next period.

4.5.2 Precipitation data and distribution

The most challenging object of hydrological simulation of a mountain basin is the measurement of meteorological variables. The major problems posed in high mountain areas are the accessibility to the mountains on a continuous basis, the accuracy of measured meteorological variables, and the areal representativeness of measurements (Panagoulia, 1992). It has been observed that the most important factor in accurate estimation of snowmelt runoff is the assumptions of the spatial distribution and form of precipitation. In a distributed model, it is very essential to distinguish between rain and snow in each elevation band because these two form of precipitation behaves very differently in terms of contribution to the streamflow. Rainfall is contributed faster to the streamflow whereas snowfall is stored in the basin until it melts. The form of precipitation is influenced by two factors; meteorological and topographical. Meteorological factor includes air temperature, lapse rate, wind etc and topographical factors include elevation, slope, aspect, vegetation cover etc. Snow falling through warmer atmosphere or melting level air temperature melts and falls as rain. Similarly, snow falls at elevation above melting level and rain falls at elevation below melting level.

For the present study, the daily precipitation data were available for six stations within the study area namely Darabshal, Sirshi, Bhadarwah, Hawal, Mau and Koksar as shown in (Table 4.1). The basin is divided into 9 elevation bands with an altitude difference of 600 m for convenience.

Table 4.1: Raingauge stations used for different bands

Band	Elevation range(m)	Raingauge station	Temperature (From Beas basin)
1	600-1200	Darabshal	Pandoh
2	1200-1800	Sirshi	Bhunter
3	1800-2400	Bhadarwah	Largi
4	2400-3000	Hawal	Manali
5	3000-3600	Mau	Manali
6	3600-4200	Koksar	Manali
7	4200-4800	Koksar	Manali
8	4800-5400	Koksar	Manali
9	>5400	Koksar	Manali

The rain gauge has been assigned to the different bands based on its proximity to the respective band according to altitude of the station. A critical temperature, T_c , is specified in the model to determine whether the measured precipitation is rain or snow. In the present study, T_c is considered to be 2°C as suggested by Singh and Jain, 2003. The algorithm used in the model to determine the form of precipitation is as follows:

If $T_m \geq T_c$, all precipitation is considered as rain

If $T_m \leq 0^\circ\text{C}$, all precipitation is considered as snow

Where,

T_m is mean air temperature. In the cases $T_m \geq 0^\circ\text{C}$ and $T_m \leq T_c$, the precipitation is considered as a mixture of rain and snow and their proportion is determined as follows:

$$\text{Rain} = \frac{T_m}{T_c} \times P \quad (4.5)$$

$$\text{Snow} = P - \text{Rain} \quad (4.6)$$

Where,

P is the total observed precipitation.

4.5.3 Degree days

Degree-days are the departures of temperature above or below a particular threshold value. Generally a threshold temperature of 0°C is used, with snowmelt considered to have occurred if the daily mean temperature is above 0°C. This follows from the idea that most snowmelt results directly from the transfer of heat from the air in excess of 0°C. The difference between the daily mean temperature and this threshold value is calculated as the degree-day. Snowmelt-runoff models, which incorporate a degree-day or temperature index, routine are the most commonly used in operational hydrology and have been successfully, verified world-wide over a range of catchment sizes, physical characteristics and climates (WMO, 1986; Bergstrom, 1992; Rango, 1992, Davies, 1997). An early application of a degree-day approach was made by Finsterwalder and Schunk (1887) in the Alps and since then this approach has been used widely all over the world for the estimation of snowmelt (Martinec et al., 1994; Quick and Pipes, 1995). The basic form of the degree-day approach is:

$$M = D (T_{\text{air}} - T_{\text{melt}}) \quad (4.7)$$

Where,

M = daily snowmelt (mm/day)

D = degree-day factor ($\text{mm } ^\circ \text{C}^{-1} \text{ day}^{-1}$)

T_{air} = index air temperature ($^\circ\text{C}$)

T_{melt} = threshold melt temperature (usually, 0°C)

Although air temperature and other hydrological variables vary continuously throughout the day, the daily mean air temperature is the most commonly used index temperature. When daily maximum (T_{max}) and minimum (T_{min}) air temperature is available, daily mean air temperature is calculated as

$$T_{\text{air}} = T_{\text{mean}} = \frac{(T_{\text{max}} + T_{\text{min}})}{2} \quad (4.8)$$

4.5.4 Degree Day Factor

The degree-day method is popular because temperature is a reasonably good measure of energy flux, and, at the same time, it is a reasonably easy variable to measure, extrapolate, and forecast (Martinez and Rango, 1986). The degree-day factor, D , is an important parameter for snowmelt computation and converts the degree-days to snow melt expressed in depth of water. D is influenced by the physical properties of snowpack and because these properties change with time, therefore, this factor also changes with time. The seasonal variation in melt factor is well illustrated by the results obtained from the study reported by Anderson (1973); the lower value being in the beginning of melt season and higher towards the end melt season. A wide range of a values has been reported in the literature with a generally increase as the snowpack ripens. Singh and Kumar (1996) determined the D factor by monitoring a known snow surface area of the snow block within the snowpack at an altitude of about 4000m in the western Himalayan

region in the summer. The mean daily value of the D was computed to be 5.94 mm °C-1 day-1, while for a dusted block it increased to 6.62 mm °C-1 day-1. In glacierized basins, the degree-day factor usually exceeds 6 mm °C-1 d-1 towards the end of summer when ice becomes exposed. As discussed above that D changes with season, therefore, when using degree-day approach, changes in D with season should be taken into account. In the present study in the starting of melt season for every month low value of degree-day factor has been taken and it go on increasing till the end of melt season i.e. the month of September. The range of the values of degree-day factors used in this study is given Table 4.2.

Table 4.2:Parameter values used in calibration of model

S. No.	Parameter	Symbol	Value
1.	Degree-day factor	D	1.0 – 4.0 mm.°C ⁻¹ .day ⁻¹
2.	Runoff coefficient for rain	C _r	0.40 - 0.70
3.	Runoff coefficient for snow	C _s	0.50 – 0.80
4.	Temperature lapse rate	δ	Seasonally varying
5.	Critical temperature	T _c	2°C
6.	Number of linear reservoirs for snow free area	N _r	2
7.	Number of linear reservoirs for snow covered area	N _s	1
8.	Number of linear reservoirs for subsurface flow	N _b	1

4.5.5 Rain on snow

Rain-on-snow event is hydrologically an important phenomenon as most of the floods in British Columbia, Washington, Oregon and California were reported to have occurred due to this event (Colbeck, 1975; Kattelmann 1987; Brunengo, 1990; Berg et al., 1991; Archer et al., 1994). Further, this event is one of the prime causes of avalanches as rain falling over snow weakens the bond between the snowpacks thereby reducing the mechanical strength of the snowpack (Conway et. al, 1988; Heywood, 1988; Conway and Raymond, 1993). When rain falls on snowpack it is cooled to the temperature of snow. The heat transferred to the snow by rainwater is the difference between its energy content before falling on the snow and its energy content on reaching thermal equilibrium within the snowpack. For snowpacks isothermal at 0°C, the release of heat results in snowmelt, while for the colder snowpack this heat tends to raise the snowpack temperature to 0°C. In case the snowpack is isothermal at 0°C, the melt occurring due to rain is computed by (Jain, 2001)

$$M_r = \frac{4.2 T_r P_r}{325} \quad (4.9)$$

Where,

M_r = melt caused by the energy supplied by rain (mm/day)

T_r = temperature of the rain (°C)

P_r = depth of rain (mm day⁻¹)

Only high rainfall events occurring at higher temperatures would cause the melting due to rain, otherwise this component would not be significant (Singh et al., 1997).

4.5.6 Computation of different runoff components

The streamflow from a snowfed river has three components namely,

- runoff from the snow-covered area,
- runoff from snow free-area and
- baseflow

The runoff contributed from all the three components are computed separately for each elevation band and the output from all the bands are integrated to provide the total runoff from the basin.

4.5.6.1 Surface runoff from snow covered area

Runoff contributed from snow-covered area consists of

- Snowmelt triggered by the increase in air temperature above melting temperature
- Under rainy conditions, melt caused by the heat transferred to the snow surface by the rain
- Runoff from the rain itself falling over snow covered area

(a) Snowmelt caused by the increase in air temperature has been estimated by degree-day approach. In this approach degree-day factor is used to convert degree-day into snow expressed in depth of water.

$$M_{s,i,j} = C_{s,i,j} D_{i,j} T_{i,j} S_{c,i,j} \quad (4.10)$$

Where,

$M_{s,i,j}$ = snowmelt on i^{th} day for j^{th} band (mm)

$C_{s,i,j}$ = coefficient of runoff for snow on i^{th} day for j^{th} band

$D_{f,i,j}$ = degree-day factor on i^{th} day for j^{th} band ($\text{mm} \cdot ^\circ\text{C}^{-1} \text{d}^{-1}$)

$T_{i,j}$ = temperature on i^{th} day for j^{th} band ($^\circ\text{C}$)

$S_{c,i,j}$ = Ratio of snow covered area to the total area of j^{th} band on i^{th} day

- (b) Runoff depth from the snowmelt contributed by the heat transferred from rain falling over a snow pack is given by the equation described in section 6.5.7

$$M_{r,i,j} = \frac{4.2 T_{i,j} P_{i,j} S_{c,i,j}}{325} \quad (4.11)$$

where,

$M_{r,i,j}$ = snowmelt due to rain on snow on i^{th} day for j^{th} band (mm)

$P_{i,j}$ = rainfall on snow on i^{th} day for j^{th} band (mm)

- (c) Runoff depth from rain itself falling over the snow-covered area, R_s , is given by

$$R_{s,i,j} = C_{s,i,j} P_{i,j} S_{i,j} \quad (4.12)$$

For the computation of runoff from rain, the coefficient C_s is used (not the rainfall runoff coefficient, C_r), because the runoff from the rain falling on the SCA behaves like the runoff from the melting of snow.

The daily total discharge from the SCA is computed by adding the contribution from each elevation zone. Thus, discharge from the SCA, Q_{SCA} , for all the zones are given by:

$$Q_{SCA} = \alpha \sum_{j=1}^n (M_{s,i,j} + M_{r,i,j} + R_{s,i,j}) A_{SCA,i,j} \quad (4.13)$$

Where,

n = total number of zones

A_{SCA} = snow-covered area (km^2) in the j^{th} zone on the i^{th} day

α = factor (1000/86400 or 0.0116) used to convert the runoff depth (mm day^{-1}) into discharge ($\text{m}^3 \text{s}^{-1}$).

This discharge is routed to the outlet of the basin following the procedure described in the next section.

4.5.6.2 Surface runoff from snow-free area

The only source of surface runoff from snow-free area (SFA) is rainfall. Like snowmelt runoff computations, runoff from the SFA was computed for each zone using the following expression:

$$R_{f,i,j} = C_{r,i,j} P_{i,j} S_{f,i,j} \quad (4.14)$$

where,

$C_{r,i,j}$ = coefficient of runoff for rain on i^{th} day for j^{th} band

$P_{i,j}$ = rainfall on snow on i^{th} day for j^{th} band (mm)

$S_{f,i,j}$ = Ratio of snow free area to the total area of j^{th} band on i^{th} day.

Because SCA and SFA are complimentary to each other, $S_{f,i,j}$ can be directly calculated as $1 - S_{c,i,j}$. The total runoff from SFA, Q_{SFA} for all the zones is thus given by:

$$Q_{SFA} = \alpha \sum_{j=1}^n R_{f,i,j} A_{SFA,i,j} \quad (4.15)$$

Where, $A_{SFA,i,j}$ = snow-free area in the j^{th} zone on the i^{th} day

The discharge from the SFA was also routed to the outlet of the basin before adding it to the other components of discharge.

4.5.6.3 Subsurface runoff

The subsurface flow or baseflow represents the runoff from the unsaturated zone of the basin to the streamflow. After accounting for the direct surface runoff from snowmelt and rainfall, the remaining water contributes to the groundwater storage through infiltration and appears at the outlet of the basin with much delay as subsurface flow or baseflow. Depletion of this groundwater storage also results from evapotranspiration and percolation of water to the deep groundwater zone. It is assumed that half of the water percolates down to shallow groundwater and contributes to baseflow, while the rest is accounted for by the loss from the basin in the form of evapotranspiration and percolation to the deep groundwater aquifer, which may appear further downstream or become part of deep inactive groundwater storage. The depth of runoff contributing to baseflow from each zone is given by:

$$R_{b,ij} = \beta[(1 - C_{r,ij})R_{f,ij} + (1 - C_{s,ij})M_{t,ij}] \quad (4.16)$$

Where,

$$M_{t,ij} = M_{s,ij} + M_{r,ij} + R_{s,ij} \text{ and } \beta \text{ is } 0.50.$$

The baseflow, Q_b , is computed by multiplying the depth of runoff by the conversion factor α and area, and is given as:

$$Q_b = \alpha \sum_{j=1}^n R_{b,ij} A_{ij} \quad (4.17)$$

Where,

A is the total area (km^2) and represents the sum of A_{SCA} and A_{SFA} . This component is also routed separately.

4.5.6.4 Total runoff

The daily total streamflow from the basin is calculated by adding the three different routed components of discharge for each day.

$$Q = Q_{sca} + Q_{sfa} + Q_b \quad (4.18)$$

As discussed above, the direct runoff results from overland or near surface flow, while baseflow is regarded as being a result of groundwater contribution into the stream. Infact, the contribution to baseflow starts only after the topsoil is saturated. In order to consider the soil moisture deficit, soil moisture index (SMI) has been considered in the present study. The routing of surface and subsurface runoff has been carried out separately and described in the following sections.

4.5.7 Routing of different components of runoff

4.5.7.1 Routing of surface runoff

The catchment routing is the transformation of input to the basin either in the form of rainfall, snowmelt or baseflow to the outflow from the basin. Since the hydrological response of SCA and SFA are different, routing of runoff from these areas was done separately. The linear cascade reservoir approach was used for routing. In case, the inflow is passed through a series of linear reservoirs with equal storage coefficient, an integrated effect of all the reservoirs will be observed in the outflow from the last reservoir. The outflow of the upper reservoir is routed through the next reservoir. Considering n reservoirs in series, the outflow from the second reservoir is the inflow to the third reservoir and so on. The outflow from the n^{th} reservoir represents the response

of catchment in terms of outflow. Thus, each reservoir plays its role in affecting attenuation and lag characteristics of the outflow. The analytical version of the cascade of equal linear reservoirs is known as the Nash Model. In case of cascade of reservoirs, the outflow from the n^{th} reservoir is expressed as:

$$Q_{n+1,j+1} = C_0 Q_{n,j+1} + C_1 Q_{n,j} + C_2 Q_{n+1,j} \quad (4.19)$$

Where,

n = number of reservoirs and

j = time index

For a linear reservoir, $C_0 = C_1$, and therefore the equation representing the outflow from the n^{th} reservoir is simplified as:

$$Q_{n+1,j+1} = 2C_1 \bar{Q}_{n,j+1} + C_2 Q_{n+1,j} \quad (4.20)$$

Where,

$$\bar{Q}_{n,j+1} = \frac{Q_{n,j+1} + Q_{n,j}}{2} \quad (4.21)$$

Where,

$$C_0 = \frac{\Delta t/k}{2 + \Delta t/k} \quad (4.22)$$

$$C_1 = C_0 \quad (4.23)$$

$$C_2 = \frac{2 - \Delta t/k}{2 + \Delta t/k} \quad (4.24)$$

Here, C_0 , C_1 , C_2 are the routing coefficients and the sum of these coefficients equal unity, i.e.

$$C_0 + C_1 + C_2 = 1$$

The routing of different components of streamflow is done separately by using the equation 6.17. The total output from the basin was computed by summing the different routed components of runoff. Since snowmelt and rain has different response in SCA and SFA and varies with time, both the components were separately routed considering their respective areas, namely SCA and SFA. Each part of the basin is conceptualized as a cascade of linear reservoirs.

4.5.7.2 Routing of subsurface runoff

Subsurface runoff to channel is a very slow movement of water compared to the direct runoff. The source of subsurface flow is soil water in excess of field capacity. This excess water percolates to shallow groundwater zones or moves down slope at shallow depths from point of infiltration to some point of discharge above the water table. The subsurface runoff is routed in the same way as surface runoff with a given value of subsurface storage coefficient, k_b , which is determined using streamflow record of the recession period. The recession of baseflow was represented in the model by the exponential method given below:

$$Q_b(t) = Q_0 e^{-t/k_b} \quad (4.25)$$

Where,

Q_b = discharge at time t

Q_0 = discharge at time $t = 0$

k_b = recession constant or the depletion factor

This equation can be written in logarithmic form as:

$$\ln Q = \ln Q_0 - \frac{t}{k} \quad (4.26)$$

In order to determine the storage coefficient, k_b , for the baseflow, the streamflow of the recession period was plotted against time on semi-log paper and a best fit line was drawn, the slope of which gives the value of k_b . In the present study, to compute k_b , the recession trends of flow, the streamflow records were examined for a number of years. It was found that the minimum flow in the Chenab River was observed during the winter period. There was continuous recession of flow from the basin during this period, except for some anomalous change in the flow due to local rain events. The average value of k_b , i.e. 110 days, was finally adopted for the routing of the baseflow. Due to the slow response of subsurface flow, it is routed through a single linear reservoir.

4.5.8 Efficiency criteria of the model

Numerous statistical criteria are available for numerical evaluations of model accuracy in each single year, in a particular season of the year, or a sequence of years or seasons. In a study of snowmelt models, the World Meteorological Organization (WMO, 1986) suggests several efficiency criteria that are particularly useful for snowmelt modeling. The most important criteria for model evaluation identified in the WMO study are the visual inspection of linear scale plots of simulated and observed hydrographs. Several numerical criteria are also identified as useful for model evaluation.

The model performance on a daily basis is commonly evaluated using the non-dimensional Nash-Sutcliffe 'R²' value (Nash and Sutcliffe, 1970) as given by the equation,

$$R^2 = 1 - \frac{\left\{ \sum_{t=1}^n (Q_0 - Q_e)^2 \right\}}{\left\{ \sum_{t=1}^n (Q_0 - \bar{Q}_0)^2 \right\}} \quad (4.27)$$

Where,

R² = Nash-Sutcliffe coefficient of goodness of fit

Q₀ = daily observed discharge from the basin

Q_e = daily estimated discharge from the basin

\bar{Q}_0 = mean of observed discharge

n = number of days of discharge simulation

The value of Nash-Sutcliffe coefficient is analogous to the coefficient of determination and is a direct measure of the proportion of the variance of the recorded flows explained by the model.

The model performance on a seasonal basis can also be determined by computing the percentage volume difference between the measured and computed seasonal runoff as,

The main objective of the present study is application of snowmelt runoff model for estimation of stream flow in Chenab basin up to Premnagar. For application of snowmelt runoff model, two main input are snow cover area and temperature lapse rate. These two inputs have been prepared from satellite data. The methodology for obtaining these two inputs has been described in the previous chapter. The results obtained are discussed below. After this simulation results of the model are presented.

5.1 DIVISION OF CATCHMENT INTO ELEVATION BANDS

In the present study, the basin is divided into 9 elevation bands with an altitude difference of 600 m for convenience. The area covered in each elevation zone of the basin is given in Table 5.1. Digital Elevation Model of the study area is used for the preparation of the area-elevation curve, shown in Figure 5.1.

5.2 SNOW COVER AREA

SCA between February 2000 - December 2005 was estimated from MODIS data. The snow covered area maps in different years are shown in Figures 5.2 to 5.6. Using the classified snow maps, the total percentage of snowcover in the study area was estimated for different dates. On the basis of this information snow cover depletion curves have been drawn. The snow depletion curves for the months of April to August for years (2000-01, 2001-02, 2002-03 and 2003-04) are shown in Figure 5.7.

Table 5.1: Chenab basin area covered in different elevation band

Zones	Elevation range (m)	Area (km²)	Percentage
1	600-1200	48.69	0.28
2	1200-1800	335.92	1.98
3	1800-2400	815.51	4.81
4	2400-3000	1481.07	8.73
5	3000-3600	2195.70	12.94
6	3600-4200	3268.78	19.27
7	4200-4800	3988.58	23.51
8	4800-5400	3769.03	22.22
9	>5400	1059.61	6.25

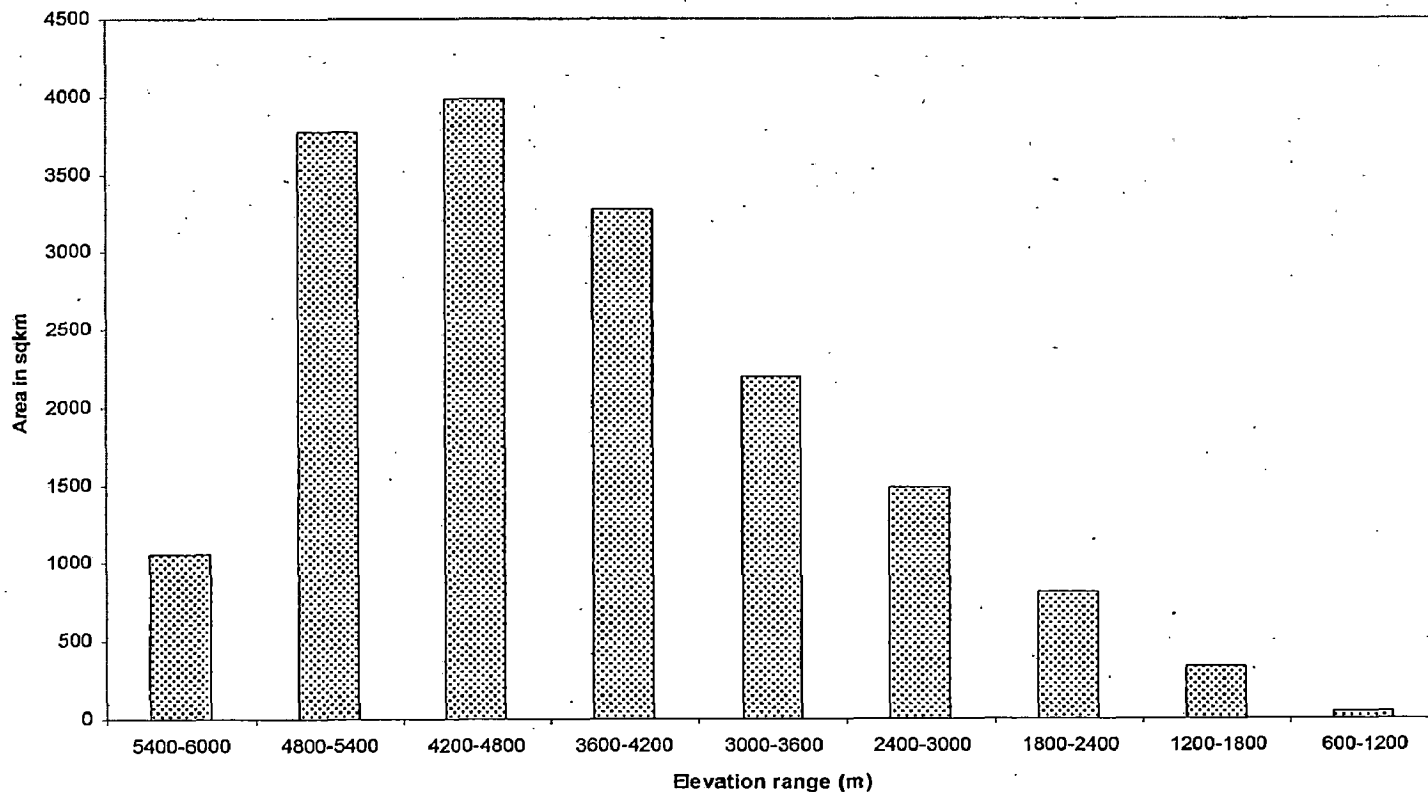


Figure 5.1: Area covered in each elevation zone of the Chenab river basin

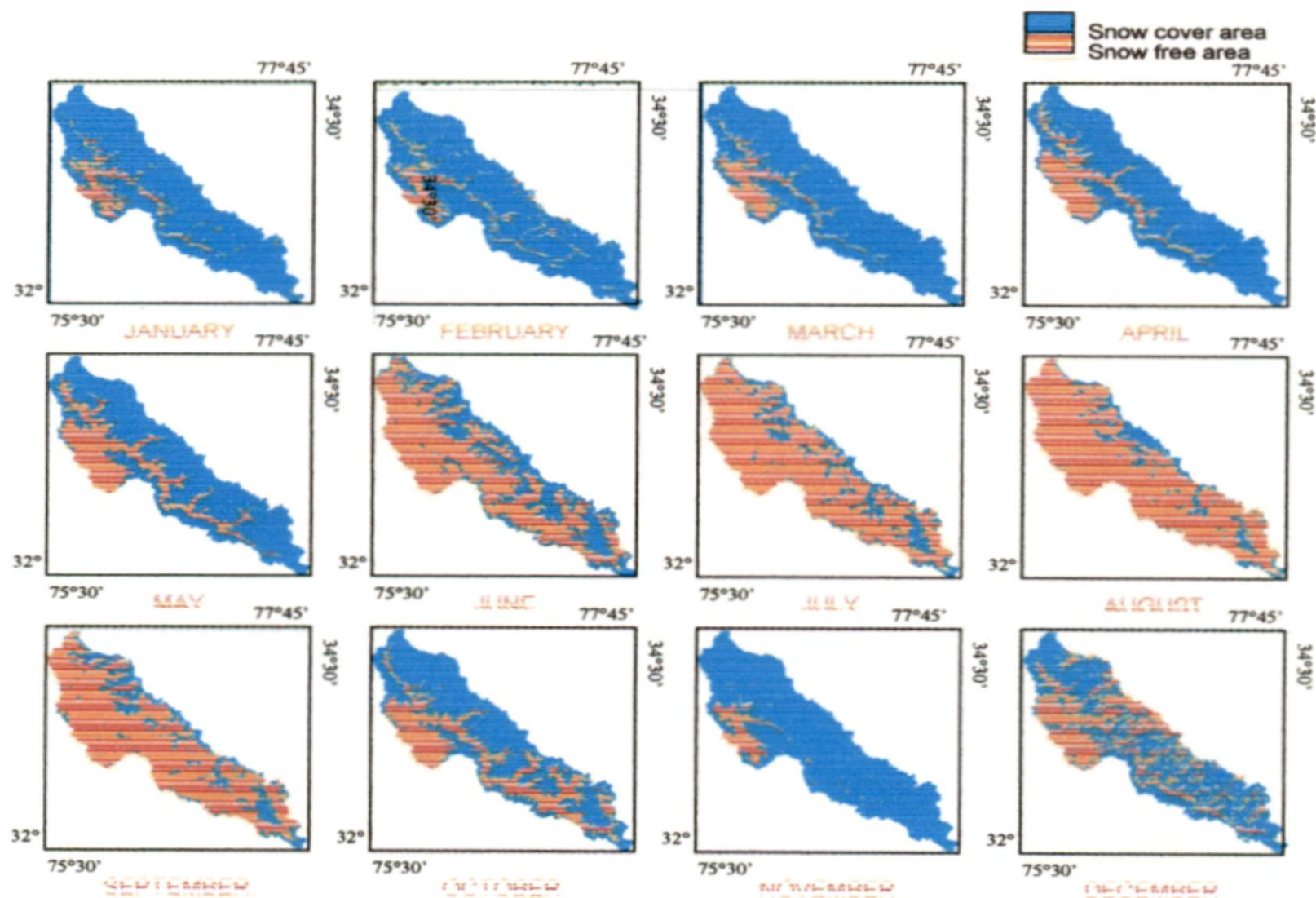


Figure 5.2 Snowcover area for the year 2001

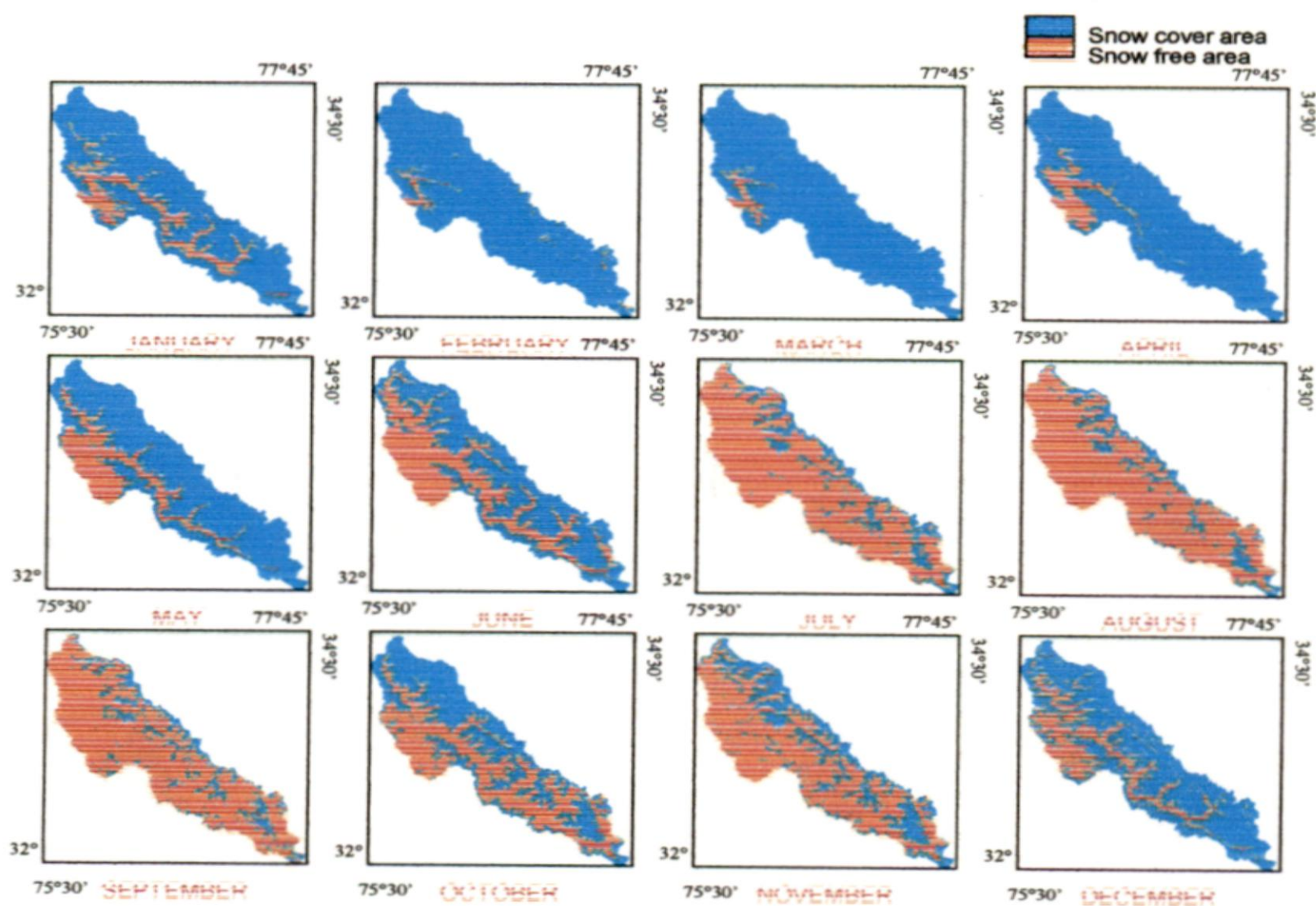


Figure 5.3 Snowcover area for the year 2002

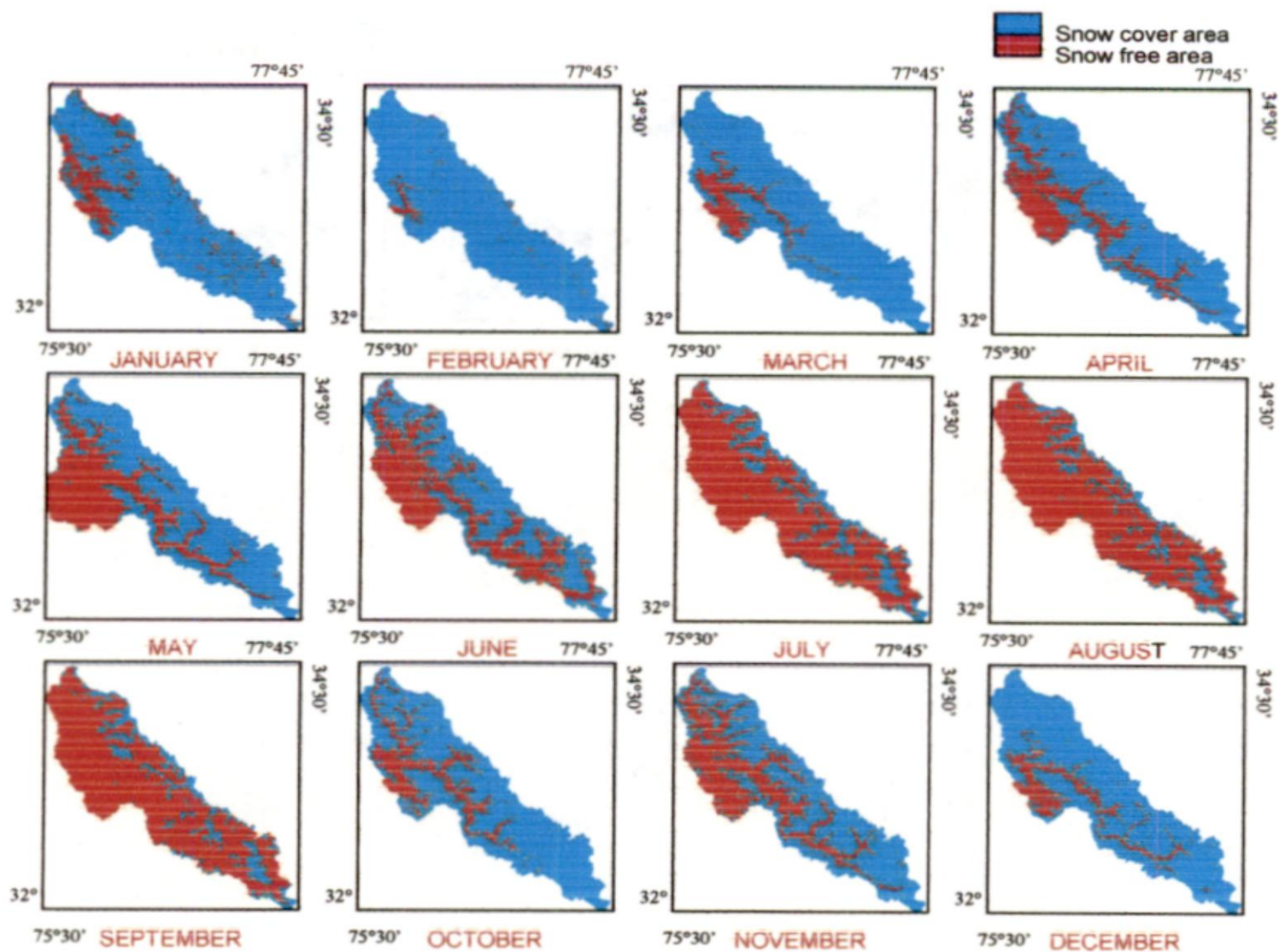


Figure 5.4 Snowcover area for the year 2003

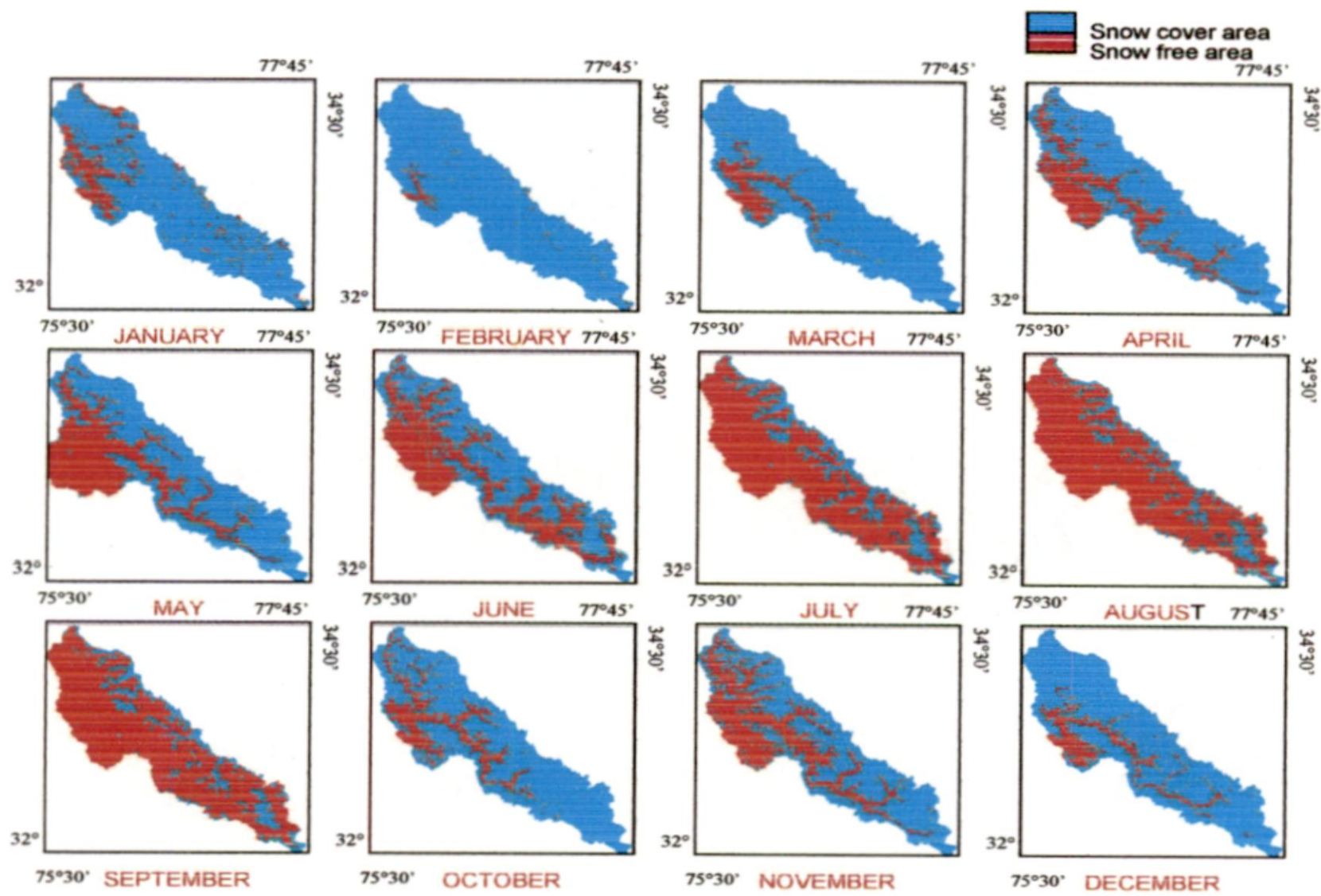


Figure 5.5 Snowcover area for the year 2004

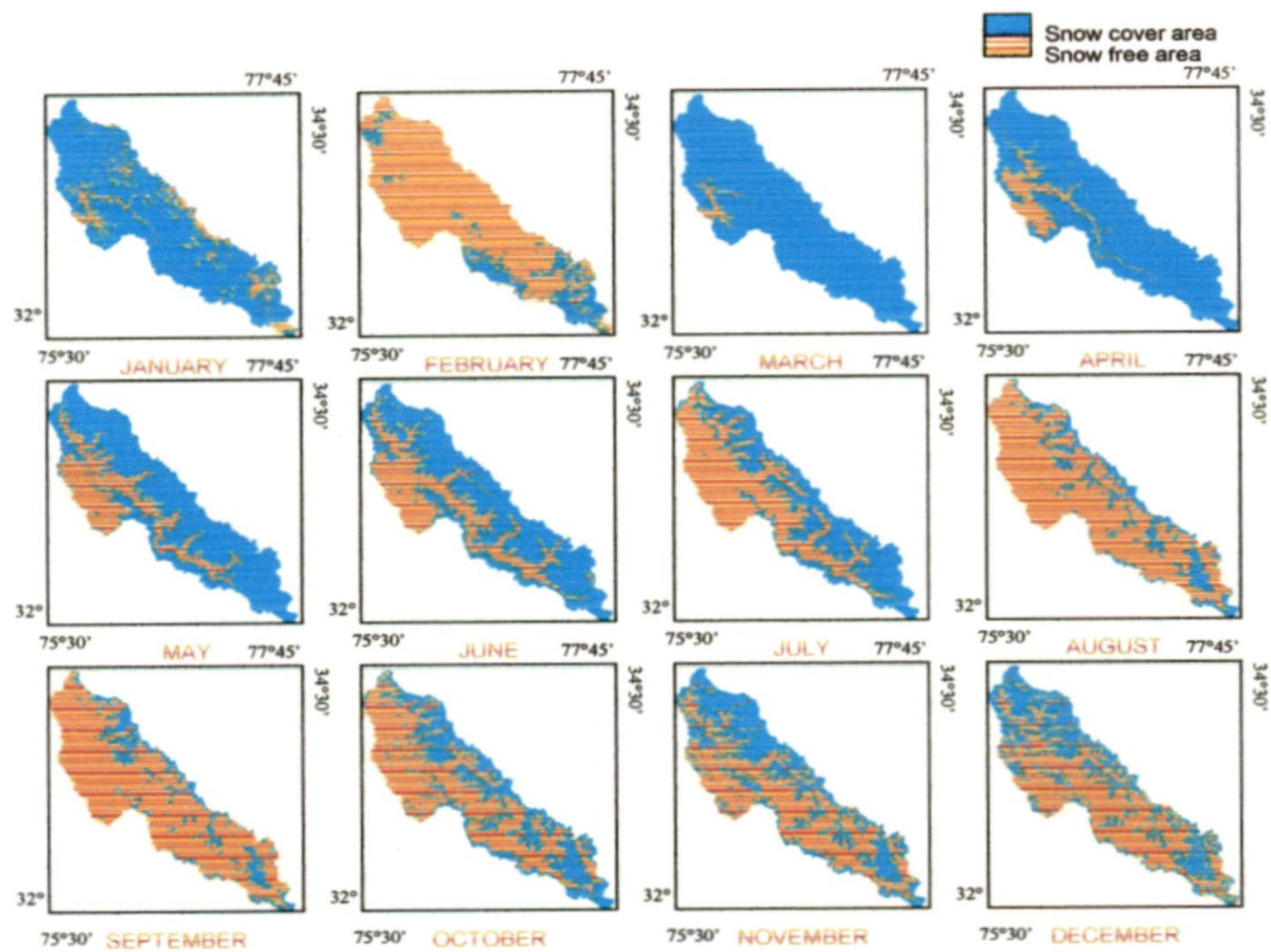


Figure 5.6 Snowcover area for the year 2005

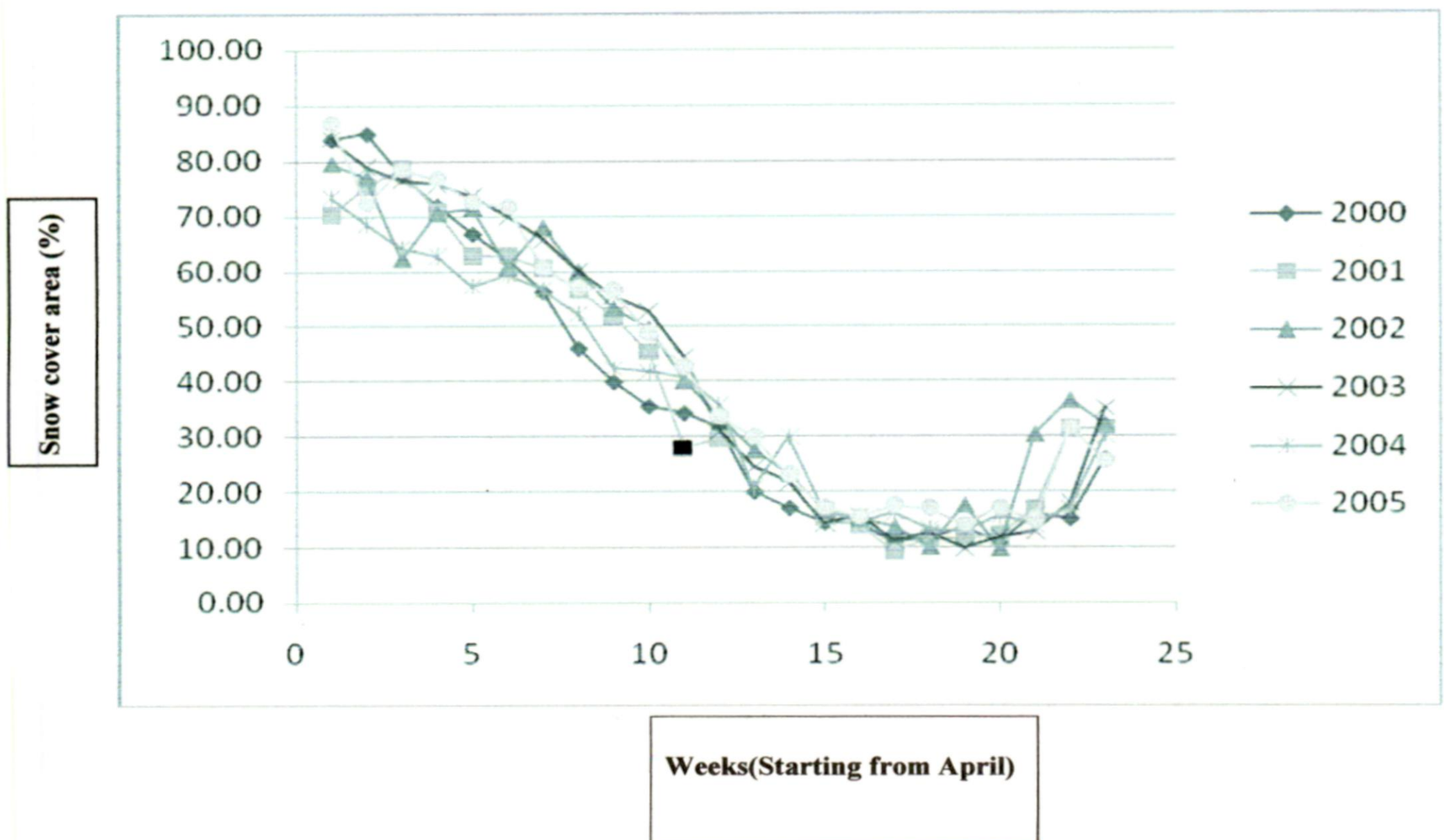


Figure 5.7: Snow cover depletion curves for Chenab basin

In the present study, the SCA has been used for different elevation zones for further application in the model. For this purpose, DEM and SCA maps have been processed for all the dates.

As discussed earlier the basin is divided into nine elevation zones. The SCA in each elevation bands were plotted against the elapsed time to construct the depletion curves for the various elevation bands in the basin for all the years. The snow cover depletion curves vary significantly from year to year and hence it has been made separately for each year under consideration. In order to simulate runoff on daily scale from the basin, daily SCA for each band was used as input to the model. The snow covered depletion in bands 4,5,6 and 7 is shown in Figure 5.8.

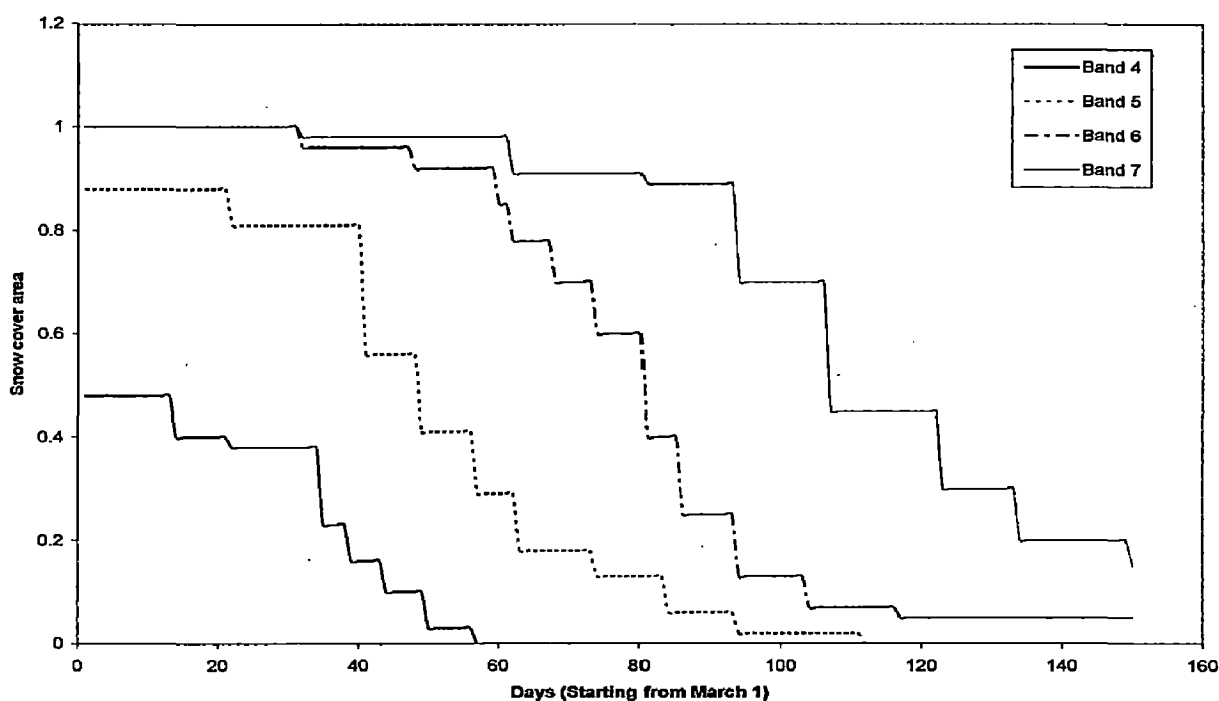


Figure 5.8 Snow covered depletion in bands 4, 5, 6 and 7

5.3 LAND SURFACE TEMPERATURE

The present study clearly demonstrates an inverse linear correlation between LST and elevation as shown in Figure 5.9.

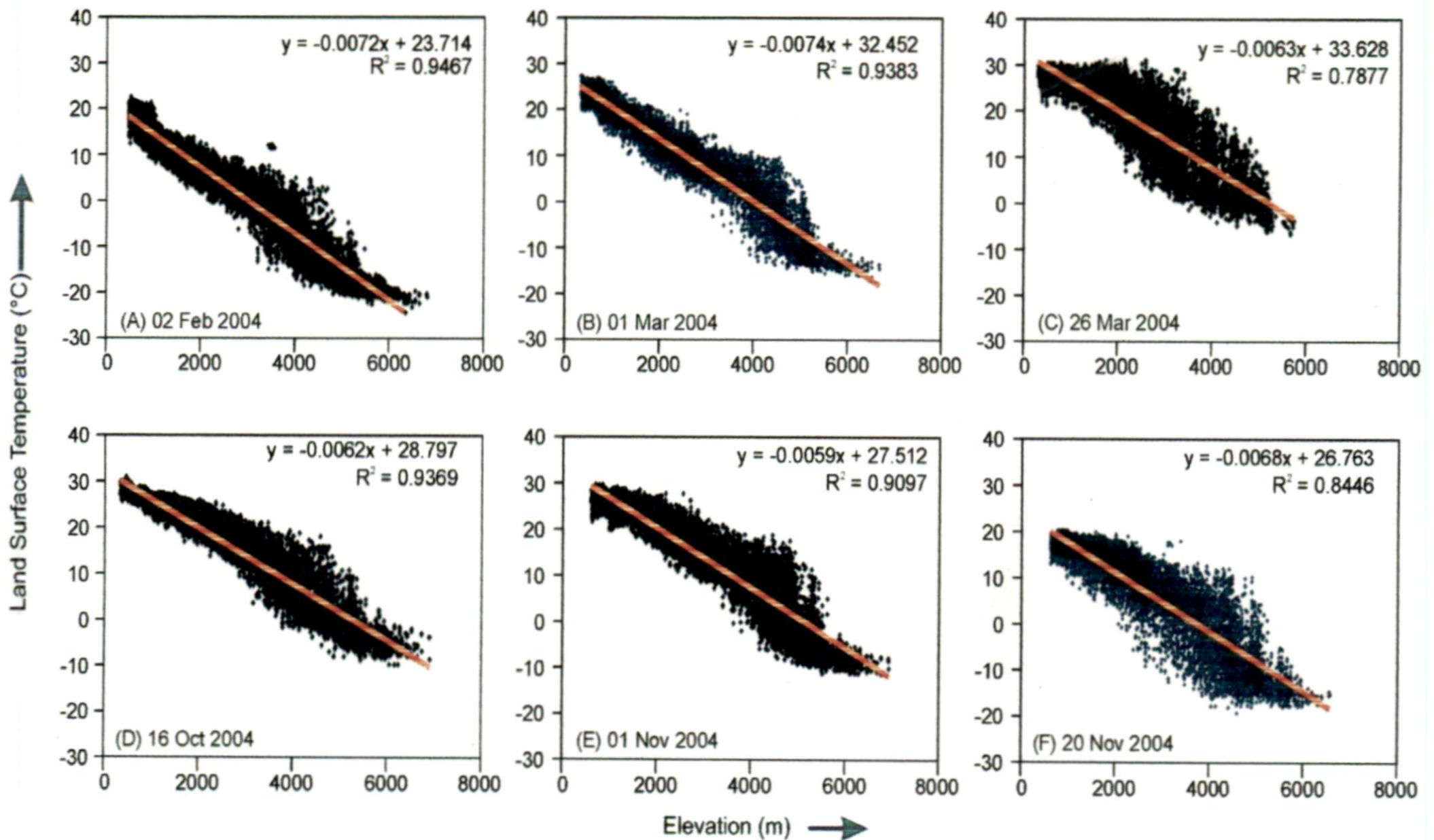


Figure 5.9: Lapse rate estimation from MODIS LST maps

The slope of the equations is the lapse rate which equals the change in LST for each unit change in elevation. Since the best fit line slope is negative, LST decreases with increase in elevation.

The results show that TLR, estimated for the study area from LST and DEM, varies between 0.40 to 0.79. The results of different months are shown in Figure 5.10. TLR is not a constant phenomena but changes with region and season. According to Bolstad et al., (1998), TLR estimated from air temperature data shows slightly

seasonal trends and averaged 4 to 10°C/km when maximum temperature is considered.

There are many advantages in estimating lapse rate using LST maps and DEM. The LST, being a continuous data, is well representative of the terrain. Being mapped by the satellite sensors, LST is readily available throughout the year except for the cloudy period. Besides, the technique of estimating the lapse rate is less time consuming.

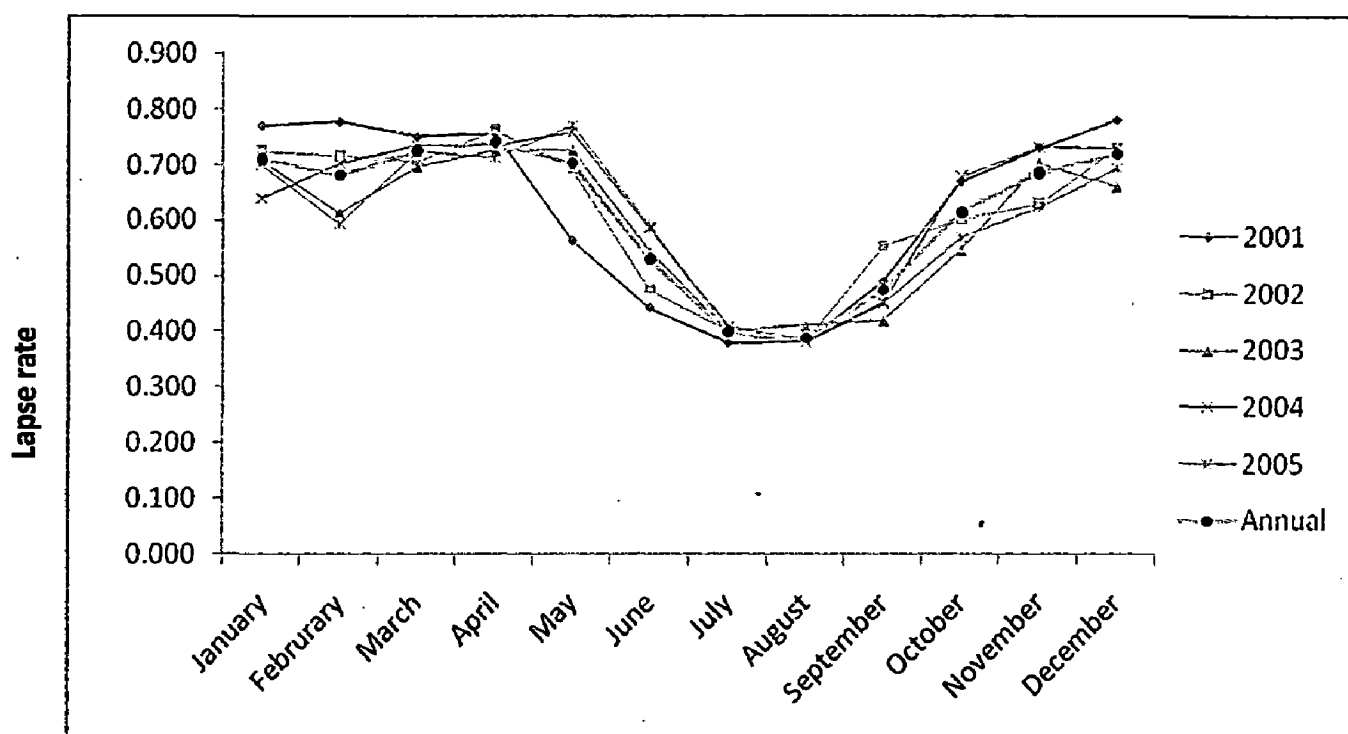


Figure5.10: Temperature Lapse rate for Chenab basin

5.4 APPLICATION OF MODEL

5.4.1 Calibration of model

The hydrological models are generally calibrated using observed and simulated results. The available data set is split into two parts; one is used for

calibration purpose and the next for validation to check how affectively the model performs in simulation mode. The calibrated parameter values were computed considering the overall performance of the model and reproduction of the flow hydrograph. For calibration three years have been considered. The results of daily streamflow simulated for the calibrated period is shown in figure 5.11, 5.12 and 5.13. In the figure five components are shown namely observed discharge, simulated discharge, contribution from snowmelt, contribution from rainfall and contribution of baseflow. From the figures 5.11 to 5.13, it can be seen that the estimated hydrograph match very well for all the years. The peaks in the inflow hydrograph are reproduced within reasonable limit.

The efficiency of the model for the calibration period is given in Table 5.2.

Table 5.2: Model efficiency during calibration period of three years

Period considered	R^2	Volume difference (%)	Root mean square error (RMSE)
2000-2001	0.91	2.13	0.55
2001-2002	0.84	7.26	0.31
2002-2003	0.92	1.57	0.46

It is noticed that for all the three years the daily discharge simulated with efficiency ranging from 0.84 to 0.92 and difference in volume ranging from 1.57% to 7.26%, which indicates good performance of the model for all the years.

5.4.2 Simulation of Streamflow

After successful calibration of the model, it was used for simulation for two independent sets of the data consisting of two years, i.e., for the year 2003-2004 and

2004-2005. The parameter estimates obtained in the calibration stage were used to simulate the runoff hydrograph for the period as mentioned above.

The simulation accuracy is determined by checking how well the model simulates the actual flow conditions. For this observed and estimated values of runoff were plotted as shown in Figures 5.14 to 5.15. From this figure it can be seen that the observed and estimated flow is correlated well and R^2 is high for both the data sets.

5.5 EFFICIENCY CRITERIA OF THE MODEL

The efficiency criteria used for comparison of model performance during simulations are given in Table 5.3 depicting difference in volume between the observed and computed flows, efficiency or coefficient of determination and root mean square errors (rmse) the model. For the two sets of period for which the simulation was performed the value of efficiency is in between 0.81-0.91 for the period 2003-2004 and 2004-2005. The difference in volume is less for all the years indicating a good match between the observed and estimated values for two independent data sets.

Table 5.3: Model efficiency during validation period of two years

Period considered	R^2	Volume difference (%)	Root mean square error (RMSE)
2003-2004	0.81	7.10	0.31
2004-2005	0.91	1.92	0.42

In all the figures, different components of total streamflow, i.e., runoff due to snowmelt, runoff due to rainfall and baseflow are shown separately. The observed and estimated hydrograph for all the years indicate very good reproduction of the flows. From the figures, it is clear that all the peaks in the outflow hydrographs are due to

rainfall. In general, the volumes and peaks are reproduced well by the model for all the years. The hydrograph recessions also fitted well but in some cases the peaks were underestimated. The contribution of snowmelt is higher especially during the pre monsoon period when there is no contribution from rainfall. Even during monsoon period the contribution from snowmelt is significant. It is well known that the baseflow sustains the flow in the stream during winter period when there is no discharge either from snowmelt or from the rainfall. The baseflow is also plotted in the figures and the reproduction of baseflow is also quite satisfactory. It can be seen that during monsoon period when there is increase in recharge due to rainfall, the trend of baseflow is also increasing.

From all the figures, it is clear that the volumes and peaks of streamflow were reproduced well by the model for all the years. The study shows that SNOWMOD a temperature index based snowmelt runoff model worked well in the study basin where limited data are available. The seasonal lapse rate was used for the first time in the model and significant improvement was observed in the efficiency of the model to simulate streamflow. The SCA estimated for the missing dates using regression method were used in the model for simulation and the efficiency of the model improved.

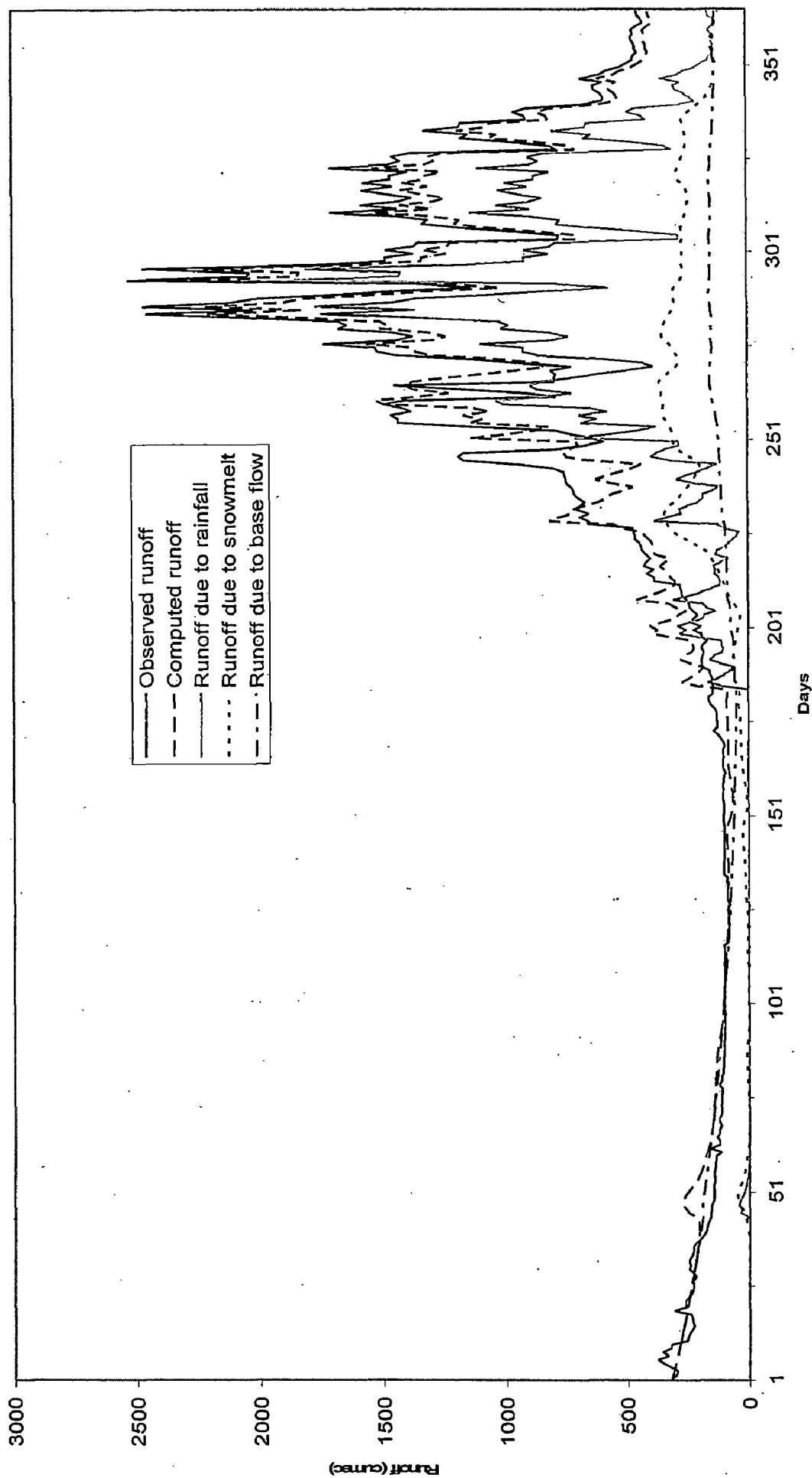


Figure 5.11 Comparison of observed and simulated hydrographs for the calibration period (2000-01) for the study area

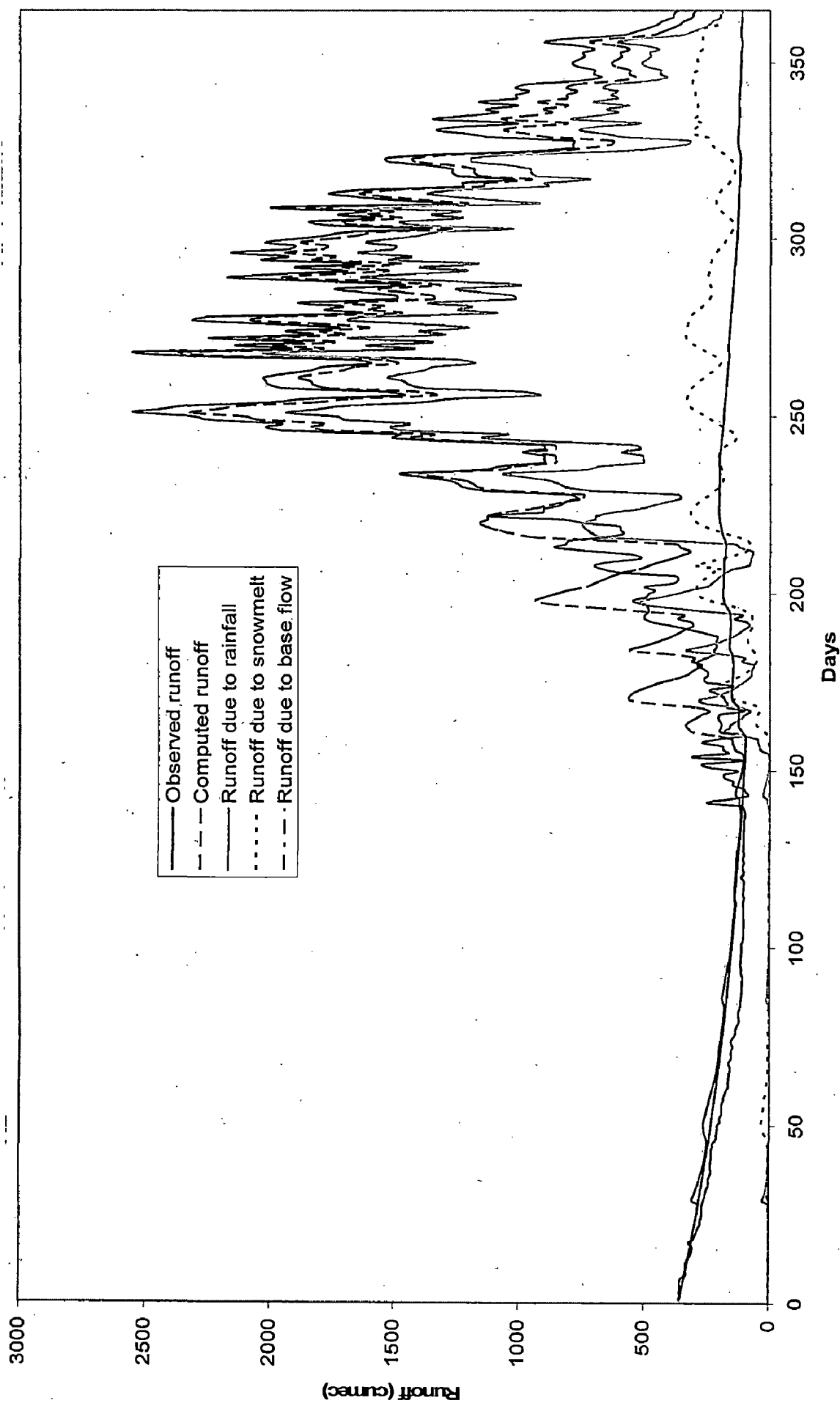


Figure 5.12 Comparison of observed and simulated hydrographs for the calibration period (2001-02) for the study area

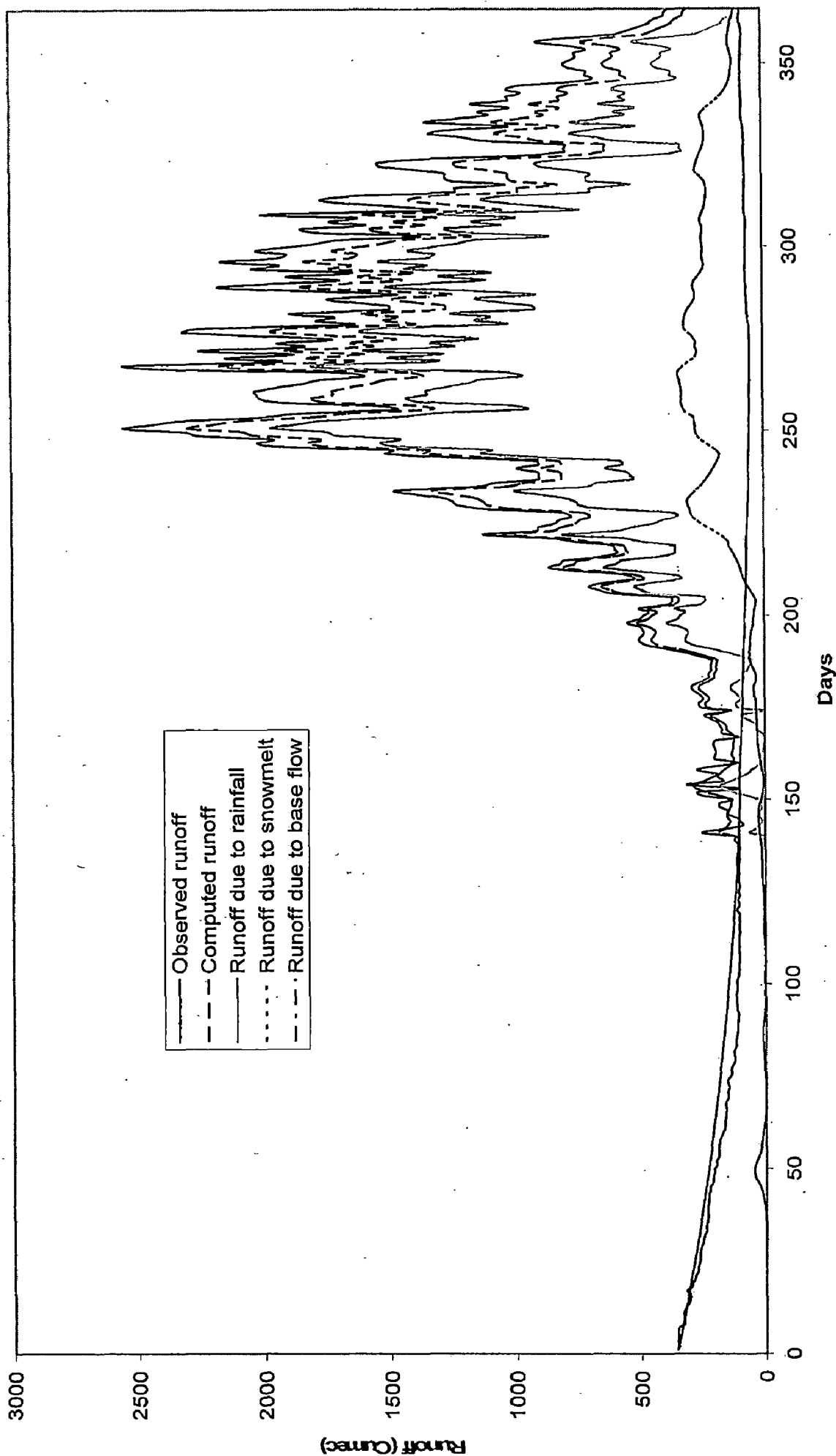


Figure 5.13 Comparison of observed and simulated hydrographs for the calibration period (2002-03) for the study area

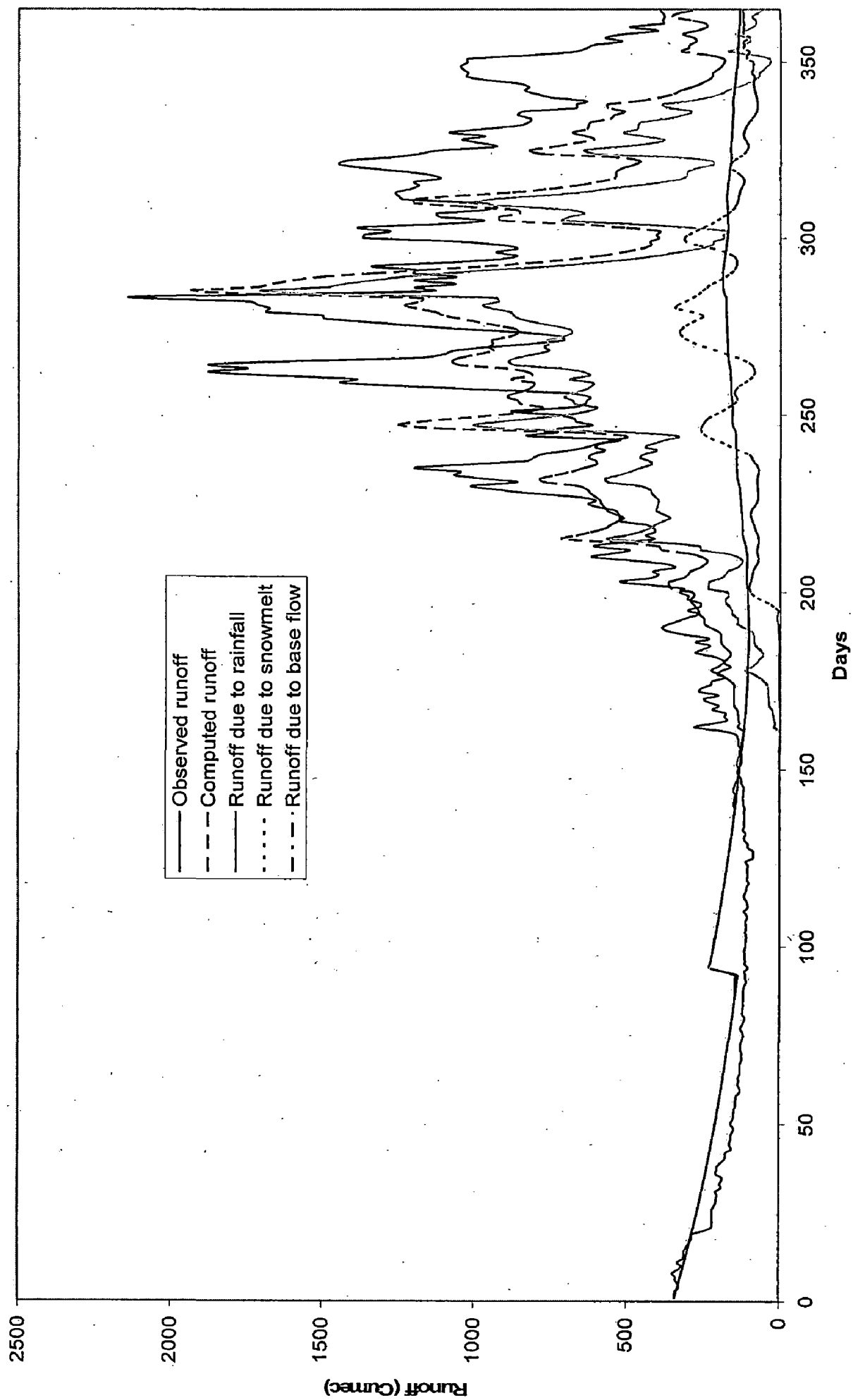


Figure 5.14 Comparison of observed and simulated hydrographs for the calibration period (2003-04) for the study area

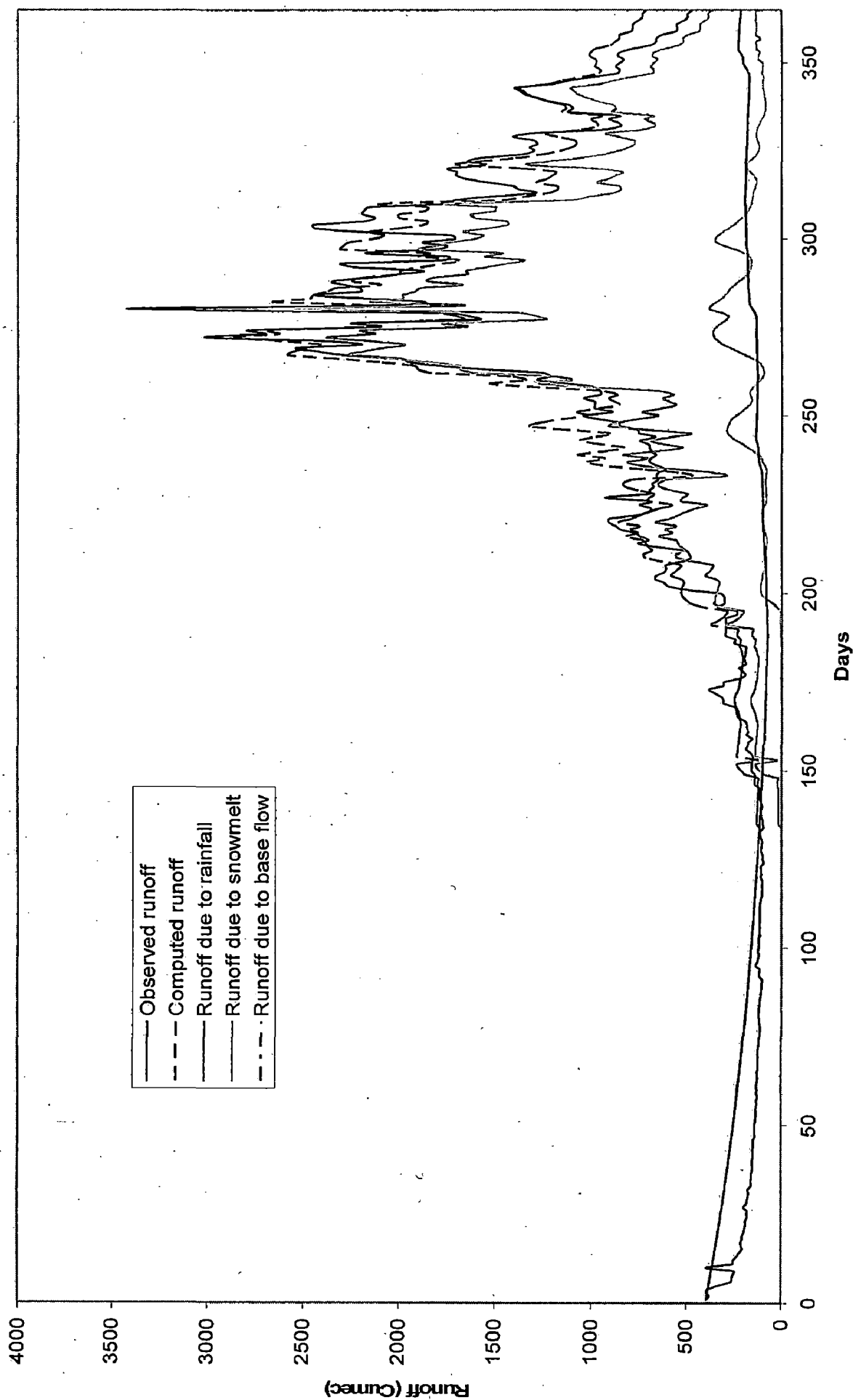


Figure 5.15 Comparison of observed and simulated hydrographs for the calibration period (2004-05) for the study area

SUMMARY AND CONCLUSIONS

CHAPTER 6

The present study has been carried out to estimate snowmelt runoff for Chenab basin up to Premnagar. For simulation of snowmelt runoff from study catchment, SNOWMOD model is used. The model requires estimates for snow covered area (SCA) and temperature lapse rate (TLR) derivable from land surface temperature (LST) estimates on daily basis. A methodology to produce daily SCA directly from Terra MODIS snows cover map products (MOD10A1) is presented. The study catchment is divided into nine elevation zones and snow cover has been computed for these elevation zones using MODIS data. On the basis of SCA, snow cover depletion curves have been prepared. It was observed that the snowmelt starts in the month of March while after August snow cover accumulation starts. The upper part of the basin remains snow covered and lower part remains snow free throughout the year. Snow covered area varies between 10% and 80% in the whole basin depending on time of the year.

In this study, LST was estimated for the Chenab river basin using split-window algorithm and lapse rate of LST was computed for five years from 2000 to 2005. The lapse rate in case of LST varies from $0.40^{\circ}\text{C}/100\text{ m}$ to $0.79^{\circ}\text{C}/100\text{ m}$. The lapse rate is maximum during winter period and is minimum during monsoon period. Therefore, the range of lapse rate obtained from the present study can be used with confidence in snowmelt runoff and other studies. This approach can be used for estimation of seasonal variation in TLR of LST. The NOAA-AVHRR images and MODIS-LST maps are freely available on Internet which makes it economically more suitable. Using available data,

the snowmelt runoff simulation is carried out for five years. Parameters of the model were calibrated using observed data for first three years and validation has been carried out for rest two years. Based on this study, following conclusions can be drawn:

1. Snow cover depletion curves vary significantly from year to year.
2. There exists an inverse linear correlation between LST and elevation.
3. SNOWMOD a temperature index based snowmelt runoff model worked well in the study basin where limited data are available.
4. During calibration period for the years 2000-2001, 2001-2002 and 2002-2003, the model efficiency obtained vary from 0.84 to 0.92 and difference in volume varied from 1.57% to 7.26% indicating good to very good performance of the model for all the years.
5. During validation period the efficiency of the model varies between 0.81-0.91, which is comparable to that achieved during calibration indicating the model can produce good simulation results on independent data sets.
6. Difference in volume is less for all the years indicating a good match between the observed and estimated values.

REFERENCES

- Anderson, E. A. (1973) The National Weather Service River Forecast System—snow accumulation and ablation model. NOAA Tech. Memo. NWS Hydro-17, National Oceanic and Atmospheric Administration, Washington DC, USA.
- Aber, J., and Federer, C., 1992, A generalized, lumped-parameter model of photosynthesis, evapotranspiration and net primary production in temperate and boreal forest ecosystems, *Oecologia*, Vol. 92, pp. 463-474.
- Baumgartner, M.F., Seidel, K., Haefner, H., Itten, K.I., and Martinec, J., 1986: Snow cover mapping for runoff simulations based on Landsat-MSS data in an alpine basin, *IAHS publication No. 160*, pp. 191-199.
- Bitner, D., T. Carroll, D. Cline, and P. Romanov. 2002. An Assessment of the Differences Between Three Satellite Snow Cover Mapping Techniques. *Hydrological Processes* 16(18):3723-3733.
- Bagchi, A.K., 1981, Snowmelt runoff in Beas basin using satellite images. PhD thesis, Department of Civil Engineering, University of Roorkee, India.
- Becker, F., and Li, Z. L., 1990, Towards a local split window method over land surfaces, *International Journal of Remote Sensing*, Vol. 11, pp. 369-393.

- Bolstad PV, Swift L, Collins F, R'eginiere RF. 1998. Measured and predicted air temperatures at basin to regional scales in the southern Appalachian Mountains. *agricultural and Forest Meteorology* 91: 161–176.
- Coll, C. and Casselles, V., 1997, A split window algorithm for land surface temperature from Advanced very high resolution radiometre data: validation and algorithm comparison, *Journal of Geophysical Research*, Vol. 102, pp 16697-16713.
- Dey, B., and Goswami, D. C., 1983, Application of Remote Sensing for seasonal runoff prediction in the Indus basin, Pakistan, *Hydrological Applications of Remote Sensing and Remote Data Transmission* (Proceedings of the Hamburg Symposium, August 1983), IAHS Publication No. 145, pp. 637-645.
- Dozier J., 1989, Spectral signature of alpine snow cover from the Landsat Thematic Mapper, *Remote Sensing of Environment* 28, pp. 9–22.
- De Scally, F.A. 1997, Deriving lapse rate of slope air temperature for melt water runoff modeling in subtropical mountains: An example from the Punjab Himalaya, *Pakisatn, Mountain Research and Development*, Vol. 17, No. 4, 353-362.
- Engman,E.T. and Gurney,R.J.,1981:*Remote Sensing in Hydrology*.Chapman and Hall,University press,Cambridge.
- Ferguson, R. I. (1999) Snowmelt runoff models. *Progr. Phys. Geogr.* 23, 205–227.
- Gupta, R. P., Duggal, A. J., Rao, S. N., Shankar, G. & Singhal, B. B. S. (1982) Snowcover area in snowmelt runoff relation and its dependence on

geomorphology—a study from Beas catchment (Himalaya, India). *J. Hydrol.* 58, 325–339.

Gupta R. P., Haritashya, U. K., and Singh, P., 2005, Mapping dry/wet snow cover in the Indian Himalayas using IRS multispectral images, *Remote Sensing of Environment*, Vol. 97, pp. 458-469.

Hall, D. K., Riggs, G. A., Salomonson, V. V., Barton, J. S., Casey, K., Chien, J. Y. L., DiGirolamo, N. E., Klein, A. G., Powell, H. W., & Tait, A. B., 2001, Algorithm theoretical basis document (ATBD) for the MODIS snow and sea ice-mapping algorithms. Available online at <http://www.modis-snow-ice.gsfc.nasa.gov/atbd01.html>.

Hall, D. K., Riggs, G. A. and Salomonson, V. V., 1995, Development of methods for mapping global snow cover using Moderate Resolution Imaging Spectrometer (MODIS) data. *Remote Sensing of Environment*, Vol. 4, pp. 127-140.

Hall, D.K. and Martinec J., 1985, *Remote sensing of ice and snow*, Chapman and Hall, London, pp. 189.

Jain, S.K. (2001) *Modeling of Streamflow and Sediment Studies in the Satluj Basin using Remote Sensing and GIS*, NIH, Roorkee, India.

Klein, A. G., Barnett, A. G., 2003, Validation of daily MODIS snow cover maps of the Upper Rio Grande River Basin for the 2000–2001 snow year, *Remote Sensing of Environment*, Vol. 86, pp. 162–176.

- Kawashima, S., Ishida, T., Minomura, M., Miwa, T., 2000, Relations between Surface Temperature and Air Temperature on a Local Scale during Winter Nights, *Journal of Applied Meteorology*, Vol. 39, pp. 1570-1579.
- Kayastha, R.B., Ohata, T. and Ageta, Y., 1999, Application of a mass balance model to a Himalayan glacier, *Journal of Glaciology*, Vo., 45, No. 151, 559-567.
- Key, J., J. A. Maslanik, T. Papakyriakou, M. C. Serreze, and A. J. Schweiger, 1994, On the validation of satellite-derived sea ice temperature, *Arctic*, vol. 47, pp. 280-287.
- Leblanc, M., Favreau, G., Maley, J., Nazoumou, Y., Leduc, C., Stagnitti, F., Oevelen, P. J., Delclaux, F., Lemoalle, J., 2006, Reconstruction of Megalake Chad using Shuttle Radar Topographic Mission data, *Palaeogeography, Palaeoclimatology, Palaeoecology*, (in press).
- Martinec, J. 1975. "Snowmelt-Runoff Model for Stream Flow Forecasts," *Nordic Hydrology*, Vol. 6, No. 3, pp. 145-154.
- NCDC, 2003, Online Document Library: Satellite Documentation. Available online at: www2.ncdc.noaa.gov/index.html.
- Riggs, G. A., Barton, J.S., Casey, K. A., Hall, D. K., & Salomonson, V. V., 2003a, MODIS Snow Products User's Guide. Available online at: http://www.snowmelt.gsfc.nasa.gov/MODIS_Snow/Sugkc2.html.

Rosen, P.A., Hensley, S., Gurrola, E., Rogez, F., Chan, S., Martin, J., Rodriguez, E.,
2001. SRTM C-band topographic data: quality assessments and calibration
activities.

Sellers, P. J., F. G. Hall, G. Asrar, D. E. Strebel, and R. E. Murphy, 1988, The first
ISLSCP Field Experiment (FIFE), Bulletin of American Meteorological Society,
Vol. 69, no. 1, pp. 22-27.

Singh, P., 1991, A temperature lapse rate study in western Himalayas. Hydrology Journal
(Indian Association of Hydrologists), 14, pp. 156–163.

Sobrino, J. A., and Raissouni, N., 2000, Toward remote sensing methods for land cover
dynamic monitoring: application to Morocco, International Journal of Remote
Sensing, Vol. 21, No. 2, pp. 353-366.

Singh, P. & Bengtsson, L. (2003) Effect of warmer climate on the depletion of snow-
covered area in the Satluj basin in the western Himalayan region. Hydrol. Sci. J.
48(3).

Singh, P., Jain, S. K. & Kumar, N. (1997a) Snow and glacier melt runoff contribution in
the Chenab River at Akhnoor Mountain Res. Devel. 17, 49–56.

Singh, P. & Kumar, N. (1996) Determination of snowmelt factor in the Himalayan
region. Hydrol. Sci. J. 41(3), 301–310.

Singh, P. & Kumar, N. (1997) Effect of orography on precipitation in the western
Himalayan region. J. Hydrol. 199, 183–206.

- Singh, P., Kumar, N. & Arora, M. (2000) Degree-day factors for snow and ice for Dokriani Glacier, Garhwal Himalayas. *J. Hydrol.* 235, 1–11.
- Singh, P. & Singh, V. P. (2001) *Snow and Glacier Hydrology*. Kluwer, Dordrecht, The Netherlands.
- Sun, G., Ranson, K.J., Kharuk, V.I., Kovacs, K., 2003. Validation of surface height from shuttle radar topography mission using shuttle laser altimeter. *Remote Sensing Environment*, Vol. 88, pp. 401–411.
- Singh, P. & Jain, S. K. (2002) Snow and glacier contribution in the Satluj River at Bhakra Dam in the Western Himalayan region. *Hydrol. Sci. J.* 47(1), 93–106.
- Tekeli, A. E., Akyurek, Z., Sensoy, A., Sorman, A. A. & Sorman, A. U., August 2005, Modelling the temporal variation in snow-covered area derived from satellite images for simulating/forecasting of snowmelt runoff in Turkey, *Hydrological Sciences Journal*, Vol. 50 , No. 4, pp. 669-682.
- Upadhyay D. S., D. K. Mishra, A. P. Johri, D. K. Mishra and A. K. Srivastava, 1991, Use of satellite based information in snowmelt run-off studies, *Mausam*, vol. 42, No. 2 pp. 187-194.
- Vogt, J.V., 1996, Land surface temperature retrieval from NOAA AVHRR data. In *advances in the use of NOAA-AVHRR data for land applications*, edited by G. D.'Souza et al., (Dordrecht, the Netherlands: Kluwer Academic Publishers) pp 125-151.

WMO (World Meteorological Organization) (1986) Intercomparison of models of snowmelt runoff. Operation Hydrology Report no. 23, WMO 646. WMO, Geneva, Switzerland.

Walland D.J. and Simmonds I. 1996. Sub-grid scale topography and the simulation of Northern hemisphere snow cover. *International Journal of Climatology* 16: 961–982.

Zhou Xiaobing B., Hongjie J. Xie, and Jan M. H. Hendrickx. 2005. Statistical Evaluation of Remotely Sensed Snow-Cover Products With Constraints From Streamflow and SNOTEL Measurements. *Remote Sensing of the Environment* 94(2):214-231.

Zhai, P., Sun, A., Ren, F., Xiaonin, L., Gao, B. and Zhang, Q., Changes of climate extreme in China. *Climatic Change*, 1999, 42, 203–218.